UNIVERSITY OF OKLAHOMA

GRADUATE COLLEGE

MECHANICAL PROPERTIES OF BABOON TYMPANIC MEMBRANE FROM YOUNG TO ADULT

A THESIS

SUBMITTED TO THE GRADUATE FACULTY

in partial fulfillment of the requirements for the

Degree of

MASTER OF SCIENCE

By

WARREN GRAHAM ENGLES
Norman, Oklahoma
2017

MECHANICAL PROPERTIES OF BABOON TYMPANIC MEMBRANE FROM YOUNG TO ADULT

A THESIS APPROVED FOR THE
STEPHENSON SCHOOL OF BIOMEDICAL ENGINEERING

BY

Dr. Rong Gan, Chair

Dr. Vassilios Sikavitsas

Dr. Chung-Hao Lee

I dedicate this paper to my mother, father, and grandmother for their support and love throughout my academic adventure.

Acknowledgements

First and foremost, I would like to thank my advisor, Dr. Rong Gan, who has inspired me over the last three years to a new level of research with the culmination of this paper. Her support has enabled me to pursue both excellence in academics as well as character development. Additionally, I would like to thank the technical and surgical assistance provided by Don Nakmali, and Kyle D. Smith. Finally, I want to thank my committee Dr. Vassilios Sikavitsas and Dr. Chung-Hao Lee for providing advice while writing my thesis.

This work was made possible by the National Baboon Research Resources at the University of Oklahoma Health Sciences Center (OUHSC) and was supported by NIH Grant Number R01DC011585.

Table of Contents

List of Tables

List of Figures

Abstract

The tympanic membrane (TM) or eardrum of the ear transfers sound waves into mechanical vibrations in the ossicular chain and into the cochlea. The mechanical properties of the TM play an important role in the sound transmission through the ear. Currently, the mechanical properties for the adult human and animal TM's are well published. However, it is unclear how age effects the mechanical properties of the TM from young to adult, and there are no published studies on pediatric models of the TM. The goal of this study is to provide the mechanical data of the baboon TM in four different age groups: less than 1 year, 1 – 3 years, 3 – 5 years, and older than 5 years of age or adult. The baboon age can be correlated to human age with a scaling factor of 1:3. With this factor the baboons that are in the first 3 groups correspond to the human pediatric age range of birth to 18 years of age, and the last group corresponds to the adult human population.

The TM specimens were prepared from baboon temporal bones, and cut into rectangle strips before mounting into the dynamic mechanical analyzer (DMA) for quasi-static and dynamic testing. The mechanical properties were obtained by measuring the stress-strain relationship, relaxation function, complex modulus at low frequencies from 1 to 80 Hz, and the failure stress and stretch ratio from young to adult baboon TMs. The adult baboon group, was additionally tested from 1 to 40 Hz at three different temperature levels: 5°C, 25°C, and 37°C. The frequency-temperature superposition (FTS) principle was used to determine complex modulus in the auditory frequency range for the adult baboon TM.

The experimental quasi-static results were further analyzed using the 1st-order hyperelastic Ogden model to derive the constitutive equations and parameters. These parameters were then used to estimate the tangent modulus for each age group of the baboon. The experimental dynamic results were used to obtain the storage and loss moduli for each age group for a frequency range from 1 to 80 Hz, and the adult baboon was obtained for a frequency range from 1 to 8000 Hz. Each baboon age group was compared to each other, and found that as the baboon ages, the stress-strain and the stiffness decreased with age. There was no change in the stress relaxation time for any age group, and there was a slight decrease in the storage and loss moduli for the low frequency range. ANOVA with Tukey-Kraemer statistical analysis was used to detect differences between the age groups, and determined that the mechanical properties of the adults were significantly lower than the younger baboons.

The quasi-static and dynamic experimental data obtained for the adult baboon TM was compared to the published human TM. The baboon average stress-strain relationship was higher than human. The stress relaxation test showed that the baboon relaxed to a higher normalized stress than the human TM. However, the complex modulus over the auditory frequency range determined by the FTS principle showed that the adult baboon's storage and loss moduli were much lower than the published human data.

The results reported in this study provide a first step towards understanding the age effect on the baboon TM's mechanical properties from young to adult.

Chapter 1: Introduction

Biomedical research is a diverse subject that pertains to various medical challenges in fields, such as biomechanics, molecular, cellular, and tissue engineering, designing biomaterials, biomedical micro- and nano-technology, bioimaging, biotransport and neural engineering. Biomechanics is mechanics applied to biology, which seeks to understand the mechanics of living systems [1]. The study of biomechanics can be on living human subjects, but these *in vivo* studies have limitations because of the non-invasive nature of the study. Current studies in auditory biomechanics require excising the tissue from the subject, stimulating, and observing the effect on the tissue in a controlled environment. This is where cadaver and animal models can be implemented to remove the ethical concern of damaging the hearing of the subject. Cadaver samples are typically sourced from the older generation of the population, but these subjects are unlikely to have the normal, healthy hearing of an adult [2]. This is where animal models with similar ear anatomy and hearing ranges can be utilized to study normal hearing at different stages of growth in the animal. These different ages can then be correlated to humans at similar stages in growth, which can enable studies to better understand the effects of age on the auditory system. These studies can include investigations into childhood impairment and middle ear infection (otitis media) a worldwide pediatric illness, which costs the healthcare system billions of dollars per year in the United States alone [2].

1.1 Ear Anatomy and Function

The human ear is a simple yet complex structure for gathering sound, amplifying or modulating, and sending the impulses to the brain for interpretation and response. Figure 1 shows the human ear anatomy and its three distinct sections: the outer, the middle, and the inner ears. The outer ear is composed of cartilaginous structures covered by squamous epithelium to form the pinna, or the visible portion of the ear. At the end of the external ear canal is the tympanic membrane (TM), which forms the boundary between the outer and middle ears. The TM plays an important role in transmitting sound from the environment to the middle ear and the inner ear. The TM is composed of three distinct layers. On the lateral side is an epidermal layer, and on the medial side is a mucosal layer. The middle layer is the fibrous stratum, which is comprised of collagen fibers, and provides stability for the TM. Within the fibrous stratum are collagen fibers that are aligned radially and concentrically around the umbo. The TM is maintained within the tympanic sulcus by the tympanic annulus, which surrounds the pars tensa. The TM is divided into two parts with the smaller portion, pars flaccida, located in the superior section of the TM, and the larger portion, pars tensa, located inferior to the neck of the malleus. Sound is converted from vibrations in the ear canal into mechanical vibrations at the TM, which travel through the ossicular chain comprised the smallest bones in the human body, the malleus, incus, and stapes, and finally into the cochlea where it is interpreted by the brain as sound [3,4].

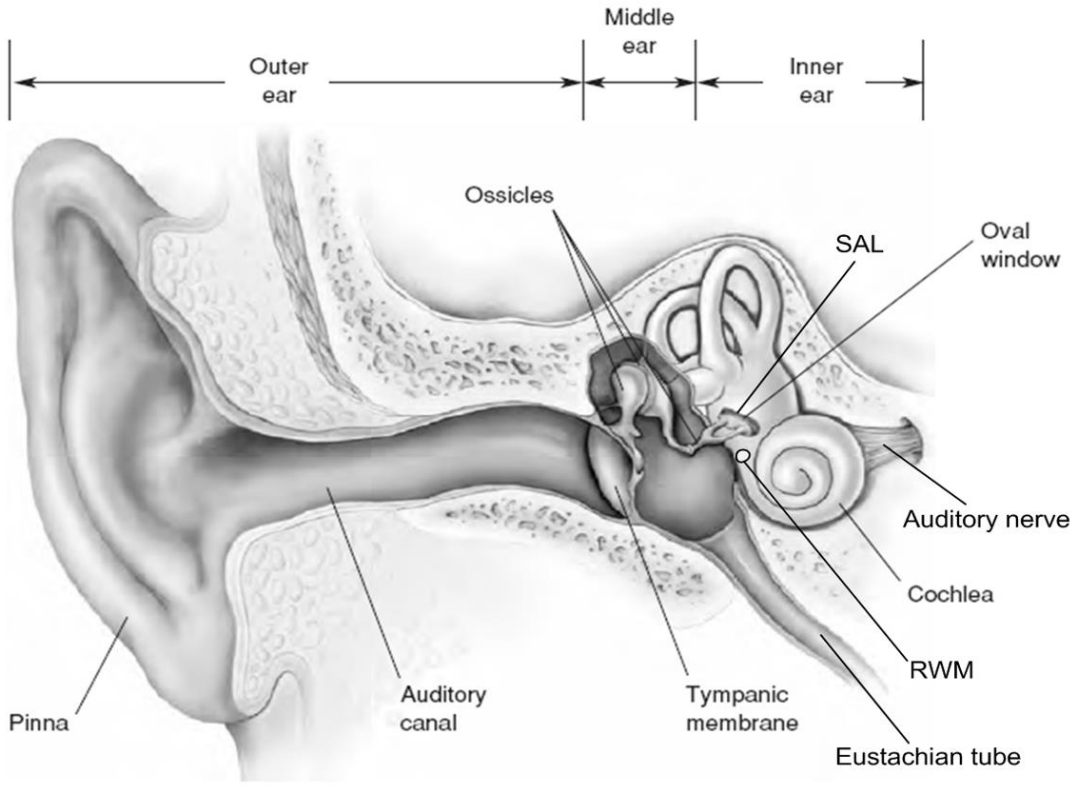

Figure 1. Ear anatomy with a complete ossicular chain and cochlea [5]

1.2 Mechanical Properties of Human Tympanic Membrane

Mechanical properties of the human TM have been characterized by numerous researchers. The static properties of the human TM were first reported by von Békésy as 20 MPa from a bending test on a rectangular cadaver TM strip [6]. Recently, a study was conducted on the human TM that focused on studying the TM under uniaxial tensile, stress relaxation, and failure tests. The experimental results were analyzed using the Ogden model and the nonlinear elastic properties were reported as a stress and stretch ratio in a stress range from 0 MPa to 1 MPa. Further investigations into the mechanical properties of human TM have been performed at the quasi-static or low frequency range [6-10]. However, the TM works under the auditory frequency range of

20-20,000 Hz, and the dynamic properties of the TM need to be measured over the auditory frequency range. Kirikae determined the Young's modulus in the circumferential direction to be 40 MPa at 890 Hz [11]. Zhang and Gan reported an investigation on the dynamic properties of the human TM using acoustic stimulation and laser Doppler vibrometry (LDV) measurements [12]. An additional publication from the same group investigated the dynamic properties of the human TM using frequency temperature superposition which directly measures the complex modulus of the TM in the frequency domain in the auditory frequency range [13]. Utilizing various techniques, the dynamic properties of the human TM in the auditory frequency range have been further characterized through the use of techniques such as the split-Hopkinson tension bar [14].

1.3 Baboon Model

The baboon is one of the largest non-hominoid members of the primate order. It is considered an African and Arabian Old World monkey belonging to the genus *Papio* [15]. Baboons are closely related to humans and have provided significant research benefits to humans in the past. The baboon shares many characteristics with humans. It is primarily bipedal which is important in regards to its anatomical relationship to the human, and thus many structures are analogous. The age of the baboon has been well studied with a correlation to human ages on a 1:3 scale [16]. For example, a 5 year old baboon is considered to be at the same stage in its life cycles as a 15 year old human. A baboon raised in captivity can live approximately 30 years, which aligns nicely with a healthy human living approximately 90 years [15]. For, this research the hearing range

of the baboon is 0.4 – 30 kHz, making it comparable to that of the human, which is 0.3 – 20 kHz.

The baboon model has been used for investigations in physiology and pathophysiology, as well as for radiopharmaceutical techniques [15]. In addition, Fourier phase analysis in radionuclide ventriculography, hemodynamic reactions in a septic shock model, and investigations in conjunction with local anesthetics (e.g., effects on cerebral blood flow) are typical examples of research that have been or are currently being performed on the baboon [15]. Recently, baboons have even been considered for stem cell based therapies in the search for a cure for Parkinson's disease [17]. Institutes using the baboon model must be adequately and ethically equipped as would be needed for investigations in human beings. Ethical considerations must be regarded strictly and supervised by an ethics committee. Protocols must determine exactly why *in vivo* experimentation is preferred to *in vitro* tests. Anesthesia techniques in a baboon model allow study on the animal itself, eliminate pain and stress to the animal, and are designed to not interfere with the aims of the investigation being performed. Finally, the baboon model is a preferred animal model in biomedical research in fertility, uterine receptivity, and embryo implantation [18,19].

Despite extensive research utilizing the baboon skull, little literature exists on baboon middle ear biomechanics. Nonhuman primate ear research has been primarily limited to ototoxicity studies, otoacoustic emissions, ionomeric prosthesis implants, and a select few publications on immunocytochemical colocalization in the cochlear nuclei [20-24]. A recent study has been done that created the first adult and infant nonhuman primate model for auditory research. However, due to the limited publications on

baboon middle ear mechanics, the model used the mechanical properties from already well established human middle ear soft tissues [25].

1.4 Applications

The mechanical properties of the TM can be implemented in a variety of applications. For example, TM grafts are used to close perforations of the membrane thereby hastening recovery, and reducing temporary hearing loss. Furthermore, the mechanical property data can be applied to finite element (FE) models of the ear to simulate sound transmission through the ear and to predict how the sound transmission would be affected by different pathologies in the ear.

Perforations of the TM result in hearing loss or deafness and possible infection due to the open communication between the air chambers of the external auditory canal and the middle ear. Perforations can result from trauma, otitis media which is an infection of the middle ear, or diseases such as cholesteatoma. For persistent perforations that do not heal spontaneously, surgical closure is usually recommended. Tympanic membrane prosthesis can be created and are most commonly of fascia or collagen sheets creating an autograft. Allografts were previously used but fell out of favor due to viral prions and the risk of human immunodeficiency virus (HIV) transmission. Surgical transplantation is therefore accomplished by placement of the graft on the medial side of the tympanic membrane to close the defect. Autograft materials include muscle fascia, perichondrium, thin cartilage slices and fat [3]. Therefore, the TM graft must close the defect, but it is critical that the materials used mimic the mechanical properties of the TM to prevent impedance of sound.

FE modeling uses elements to simplify complex problems. In general, FE reduces higher order equations into their weak form by applying nodal conditions. These conditions can then be solved iteratively to a specified convergence if an exact solution cannot be achieved [26]. This method is commonly used in many mechanical engineering applications, and has been used in a variety of biomedical engineering situations in both human and animal models [27,28]. For example, the Biomedical Engineering Laboratory at the University of Oklahoma used cross-sections obtained from histology to reconstruct the middle ear three-dimensionally (3D) as shown in Figure 2, and FE analysis was then performed to better understand sound transmission through the middle ear. In Figure 2, the research group used abbreviations C1-C7 to represent the superior (C1), lateral (C2), posterior (C3), anterior (C4) ligaments, posterior (C5), and tympani (C7) tendons [29]. This was validated by comparing the model-predicted displacement of the stapes footplate and TM with experimental measurements on human temporal bones [30]. Later the same research group applied a hyperelastic material model to the TM and other middle ear soft tissues, and a simplified two-chamber straight cochlea with basilar membrane was added to the model, which further enabled the ability to predict sound transmission from the ear canal into the cochlea [31,32]. The human FE model has been useful in predicting ear function from canal to cochlea in normal conditions, in a variety of ear pathologies, and even the behavior of implantable devices [33-35]. Recently, the first comprehensive 3D model of the adult and newborn baboon ear was developed in the Biomedical Engineering Laboratory at the University of Oklahoma. However, the FE analysis that was used on this model used mechanical property values from human experiments

because the mechanical properties for baboon middle ear structure were not yet known. While beyond the scope of this study, a future study can use the newborn and adult baboon models to better understand how sound transmission is affected by age when TM mechanical property data is applied to the FE model of the TM.

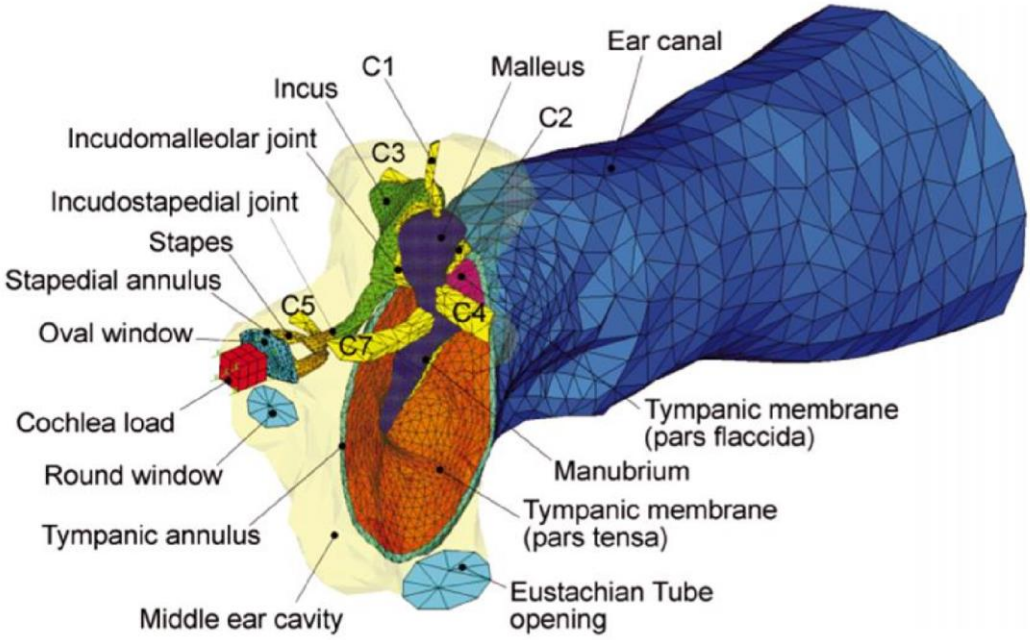

Figure 2. Human FE model of the middle ear with canal [29].

1.5 Objectives

The goal of this study is to determine the mechanical properties of the baboon TM for four different age groups: less than 1, 1 to 3, 3 to 5, and older than 5 years of age. The mechanical properties were obtained using quasi-static and dynamic testing. From this analysis, the age groups were compared to determine the effect of age on the mechanical properties of the TM. Furthermore, the mechanical data for the adult baboon group were compared to published adult human data to determine how similar the two species are with regards to the TM. Using this analysis, further research could lead to

predictions on how the human TM changes with age for assisting pediatric auditory health research.

1.5.1 Thesis Outline

Chapter 2 presents the methods used:

- 2.1 - 2.3 TM sample preparation and experimental setup
- 2.4 - 2.6 Quasi-static, dynamic, and failure testing
- 2.7 Scanning electron microscopy for adult sample
- 2.8 Statistical analysis

Chapter 3 presents results obtained from:

- 3.1 Quasi-static experimental data
- 3.2 Dynamic experimental data
- 3.3 Failure experimental data

Chapter 4 presents discussion on results:

- 4.2 Quasi-static age comparisons
- 4.3 Dynamic age comparisons
- 4.4 Adult SEM image

Chapter 2: Methods

2.1 Sample Acquisition

Fresh baboon skulls with a range of 0 days to 15 years of age from the National Baboon Research Resources at the University of Oklahoma Health Sciences Center (OUHSC) were used in this study. Using the accepted baboon to human ratio of 1:3, the youngest baboon is considered to be equivalent to a human child with an age range of 0 - 3 years of age, and the oldest baboon is considered to be equivalent to an adult human with an age approximately 45 years of age. At the National Baboon Research Resources center, the animals were evaluated post-mortem. The temporal bones were excised from the baboon skulls, and with the epithelial tissue intact. They were packed in dry ice for transit to Stephenson Technology and Research Center in Norman, Ok. The experiments were conducted within one week after arrival of the temporal bones.

The samples were processed with a solution of 0.9% saline and 15% povidone at 5°C to maintain the physiological condition before the experiment. 53 fresh temporal bones (37 females and 15 males) were involved in this study. The baboons were organized into four groups based on the age of the subject: less than 1 (G1), 1 to 3 (G2), 3 to 5 (G3), and older than 5 (G4) years of age. These groups correspond to a human age range of 0 to 3, 3 to 9, 9 to 15, and older than 45 years of age, respectively. The average age for each group was 67 ± 26 days, 2.2 ± 0.8 years, 4.2 ± 0.5 years, and 9.9 ± 3.5 years for G1, G2, G3, and G4, respectively. Summary of each samples age and the approximate human age is listed in Table 1 through Table 4. Each sample was examined under an operating microscope (OPMI-1, Zeiss, Thornwood, NY) to confirm a normal ear canal and an intact TM.

Table 1. Specimen ages in G1.

TM Specimen	Age (day)	Approx. Human Age (day)
16-9L	30	90
16-9R	30	90
17-1LP	77	231
17-1LA	77	231
17-1R	77	231
17-18L	90	270
17-18R	90	270
Mean ± SD	67 ± 26	201 ± 78

Table 2. Specimen ages in G2.

TM Specimen	Age (year)	Approx. Human Age (year)
16-8RA	1.0	3.0
16-3RP	1.5	4.5
16-4LP	1.5	4.5
16-7L	1.5	4.5
16-2LP	2.0	6.0
15-14L	2.7	8.1
17-9L	3.0	9.0
17-9R	3.0	9.0
17-11L	3.0	9.0
17-11R	3.0	9.0
Mean ± SD	2.2 ± 0.8	6.7 ± 2.4

Table 3. Specimen ages in G3.

TM Specimen	Age (year)	Approx. Human Age (year)
17-6R	3.5	10.5
17-10R	3.5	10.5
17-7R	4.0	12.0
17-2L	4.5	13.5
17-2R	4.5	13.5
17-3L	4.5	13.5
17-3R	4.5	13.5
17-4L	4.5	13.5
Mean ± SD	4.2 ± 0.5	12.6 ± 1.4

Table 4. Specimen ages in G4.

TM Specimen	Age (year)	Approx. Human Age (year)
16-6L	6.0	18.0
17-14L	9.0	27.0
17-12L	9.5	28.5
17-15L	6.0	18.0
17-16L	15.0	45.0
17-16R	15.0	45.0
17-12R	9.5	28.5
17-14R	9.0	27.0
Mean ± SD	9.9 ± 3.5	29.6 ± 10.4

2.2 Thickness Measurement with Optical Coherence Tomography

The surrounding bony wall was surgically removed, exposing the lateral surface of the TM, and the temporal bone was placed in view of the Optical Coherence Tomography (OCT). The lateral TM surface that the measurement will be read from was aligned to be normal to the laser. To reduce noise of the beam intensity, and the contrast was adjusted to create a clear image of the TM. The OCT creates an image by scanning a single point (A-scans) along a line, which are combined into the final 2D image (B-scans) seen in Figure 3.

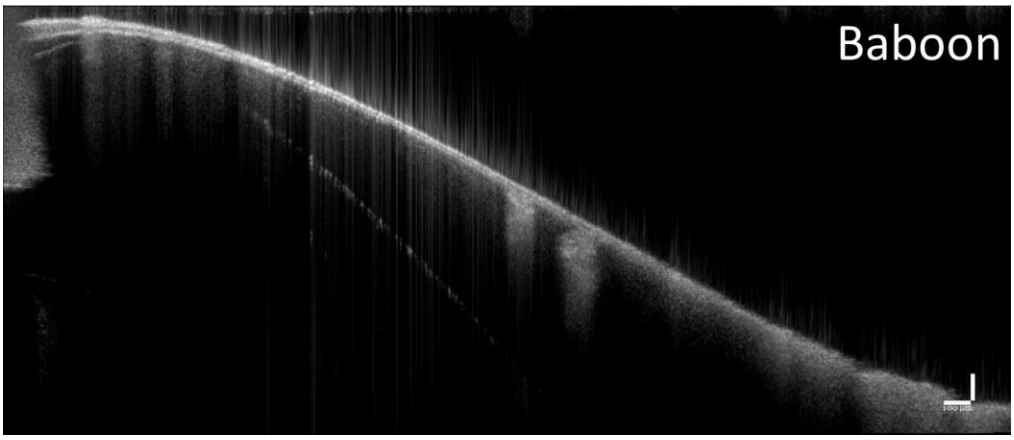

Figure 3. Example of the B-scan image obtained through OCT imaging on an intact TM within an adult baboon temporal bone.

The single point A-scans were averaged 5 times and the line scans were average 20 times. The refraction index for the TM is 1.40 and for air is 1.00 [36]. In this study, the final thickness measurement was obtained by measuring the thickness on 6 points on the entire TM surface and averaged, which neglects the non-uniformity of the thickness of the samples. The thickness for each group is reported in Table 5 through Table 8. G1 had a mean and SD of 0.025 ± 0.004 mm, G2 had a mean of 0.027 ± 0.009, G3 had a mean of 0.023 ± 0.003, and G4 had a mean of 0.024 ± 0.003.

Table 5. Thickness obtained through OCT measurement for G1.

TM Specimen	Thickness (mm)
16-9L	0.026
16-9R	0.030
17-1LP	0.020
17-1LA	0.020
17-1R	0.025
17-18L	0.024
17-18R	0.029
Mean ± SD	0.025 ± 0.004

Table 6. Thickness obtained through OCT measurement for G2.

TM Specimen	Thickness (mm)
16-8RA	0.025
16-3RP	0.020
16-4LP	0.020
16-7L	0.024
16-2LP	0.025
15-14L	0.050
17-9L	0.030
17-9R	0.030
17-11L	0.022
17-11R	0.022
Mean ± SD	0.027 ± 0.009

Table 7. Thickness obtained through OCT measurement for G3.

TM Specimen	Thickness (mm)
17-6R	0.024
17-10R	0.025
17-7R	0.022
17-2L	0.023
17-2R	0.021
17-3L	0.020
17-3R	0.022
17-4L	0.030
Mean ± SD	0.023 ± 0.003

Table 8. Thickness obtained through OCT measurement for G4.

TM Specimen	Thickness (mm)
16-6L	0.02
17-14L	0.022
17-12L	0.027
17-15L	0.029
17-16L	0.024
17-16R	0.021
17-12R	0.023
17-14R	0.025
Mean ± SD	0.024 ± 0.003

2.3 TM Strip Specimen Preparation and Experimental Setup

Figure 4 shows the TM after the ear canal and surrounding bony wall was surgically removed. The pars tensa (t), pars flaccida (f), and manubrium (*) are shown in Fig. 4, and a portion of the annulus (a) is represented as a dashed line. To remove the TM with an intact malleus first the annulus was separated from the annular sulcus, next the superior (C1), lateral (C2), anterior (C4) ligaments, the tensor tympani (C7) tendon, and the incudomalleolar joint (IMJ) were cut, and finally the TM was placed in a saline solution as shown in Fig. 5. A rectangular strip was cut from either the posterior or anterior section of the TM. The annulus was attached at the inferior and superior sides of the TM to maintain the integrity of the membrane. The TM was assumed to be a flat rectangular strip, and the curvature of the TM was neglected in this study.

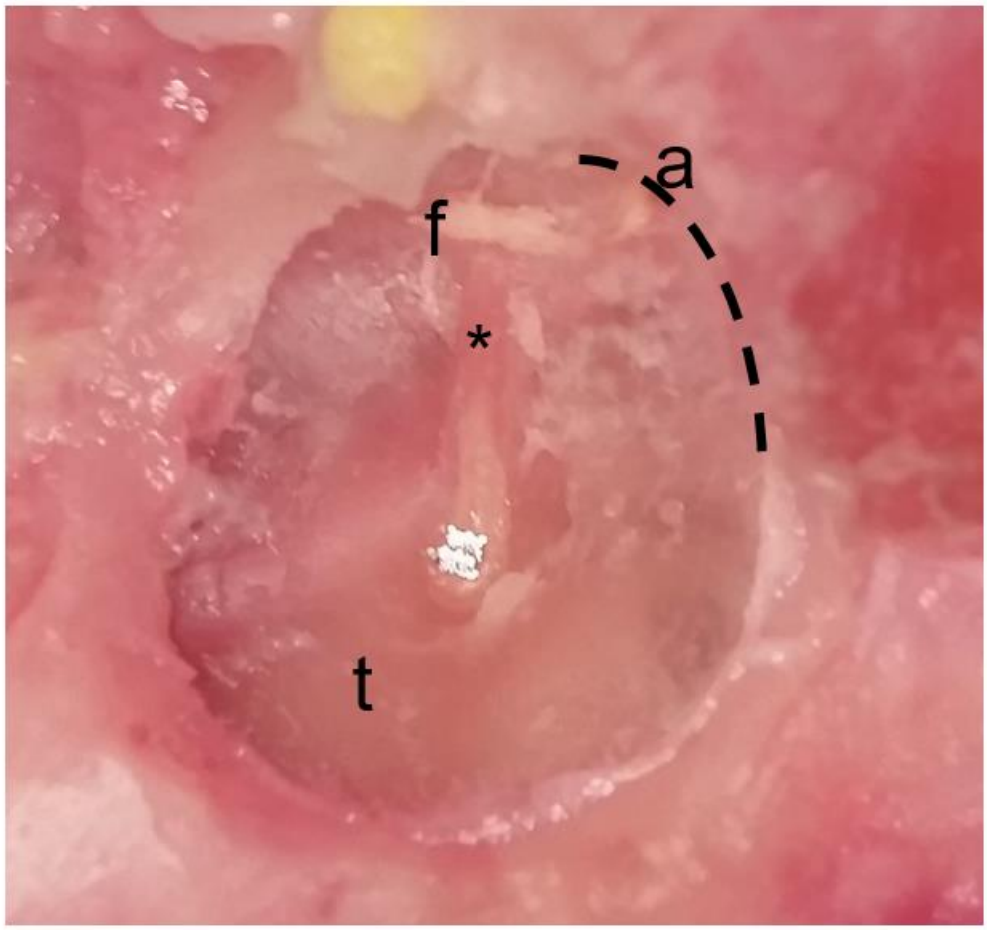

Figure 4. Intact TM within the baboon temporal bone.

A rectangular strip cut from the pars tensa of the TM was used to identify material properties. The human middle ear includes the TM or eardrum, three ossicular bones connected by two joints, and suspensory ligaments. If an intact middle ear is used to measure the material properties of the TM, a large number of unknown variables including the shape of the TM, the material properties of the malleus–incus joint, incus-stapes joint, and suspensory ligaments will be involved. To reduce the number of variables and the difficulty of parameter identification, a rectangular strip TM specimen was utilized.

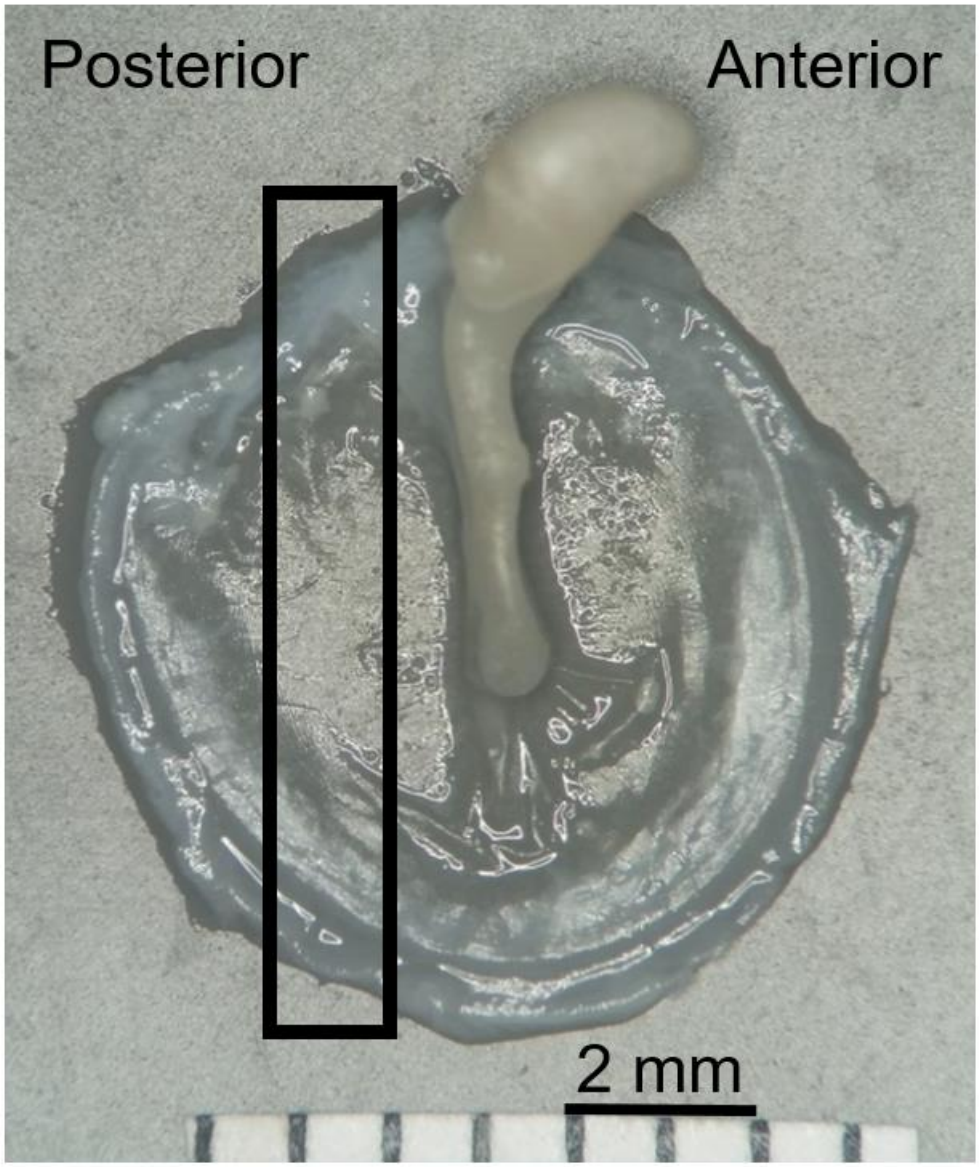

Figure 5. Typical TM sample after removing from the temporal bone. Strip samples are cut from either the posterior or anterior side indicated by the black square.

The TM strip specimen was laid on the base of a microscope (Olympus SZX12) and fixed to two aluminum fixture adapters with cyanoacrylate liquid glue (Super Glue) at both the superior and inferior annulus sides. Additionally, two plastic support braces were connected in parallel to the strip specimen between the two aluminum fixtures.

These two plastic panels were used to support the fixture adapters during the mounting process, and to avoid any unexpected damage to the TM sample throughout the mounting process. Once the specimen was aligned in the grips of the dynamic mechanical analyzer (DMA) (Bose ElectroForce 3200, Eden Prairie, MN), the support panels were cut, and a preload of 0.002 N was applied to the TM sample. Six parameters were recorded by the DMA software (WinTest 4.1, Bose, MN): elapsed time, displacement, and load, and each had a resolution of 10^{-3} sec, 10^{-3} mm, 10^{-3} N, respectively. The initial state of a mounted specimen was setup as shown in Figure 6.

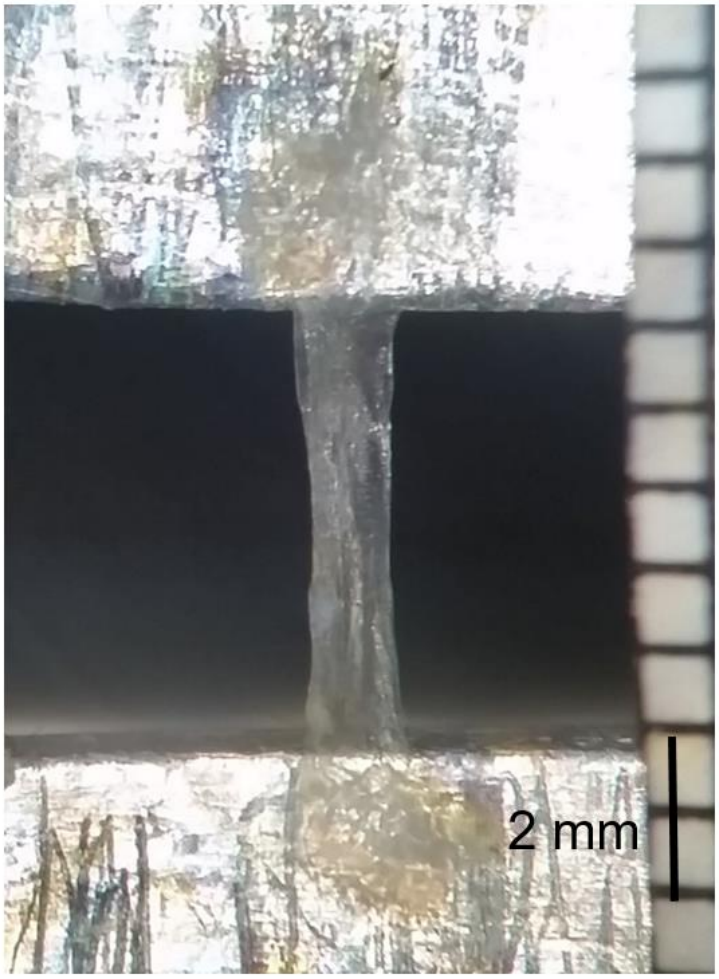

Figure 6. TM strip specimen mounted into DMA.

The length (distance between the two fixture adapters before preload) and width were measured through the microscope. The dimensions for each age group are listed in Table 9 through Table 12. The length of G1 samples ranged from 5.10 to 6.10 mm with a mean and SD of 5.64 ± 0.39 mm, and the width ranged from 1.30 to 2.10 mm with a mean of 1.80 ± 0.28 mm. The length of G2 samples ranged from 5.30 to 7.00 with a mean of 5.75 ± 0.76, and the width ranged from 1.40 to 2.10 with a mean of 1.84 ± 0.23. The length of G3 samples ranged from 4.40 to 6.30 with a mean of 5.83 ± 0.69, and the width ranged from 1.50 to 2.10 with a mean of 1.84 ± 0.23. The length of G4 samples ranged from 5.30 to 6.80 with a mean and SD of 5.68 ± 0.70, and the width ranged from 1.20 to 2.10 with a mean and SD of 1.74 ± 0.28.

Table 9. Dimensions for baboon samples for G1.

TM Specimen	Length (mm)	Width (mm)
16-9L	6.10	1.60
16-9R	5.20	1.30
17-1LP	5.10	2.10
17-1LA	5.80	2.00
17-1R	6.00	1.90
17-18L	5.80	2.00
17-18R	5.50	1.70
Mean ± SD	5.64 ± 0.39	1.80 ± 0.28

Table 10. Dimensions for baboon samples for G2.

TM Specimen	Length (mm)	Width (mm)
16-8RA	6.00	1.90
16-3RP*	5.90	2.00
16-4LP	5.30	1.50
16-7L	5.70	1.80
16-2LP*	5.50	2.00
15-14Lǂ	4.00	2.00
17-9L	6.20	1.80
17-9R	6.00	1.90
17-11L	5.90	1.40
17-11R	7.00	2.10
Mean ± SD	5.75 ± 0.76	1.84 ± 0.23

Table 11. Dimensions for baboon samples for G3.

TM Specimen	Length (mm)	Width (mm)
17-6R	5.20	1.50
17-10R	6.30	2.10
17-7R ǂ	4.40	2.00
17-2L	6.50	1.60
17-2R	6.20	2.00
17-3L	6.00	2.00
17-3R	6.00	1.60
17-4L	6.00	1.90
Mean ± SD	5.83 ± 0.69	1.84 ± 0.23

Table 12. Dimensions for baboon samples for G4.

TM Specimen	Length (mm)	Width (mm)
16-6L*	6.80	1.70
17-14L	6.40	2.00
17-12L	5.50	1.20
17-15L	5.30	1.80
17-16L	5.60	1.90
17-16R	4.50	1.60
17-12R ǂ	5.80	2.10
17-14R ǂ	5.50	1.60
Mean ± SD	5.68 ± 0.70	1.74 ± 0.28

Note: * samples were only used in low-frequency dynamic testing, ǂ samples only used in quasi-static testing, and ǂ samples only used in FTS testing.

In this study, the mechanical properties of the baboon TM for four different age groups were studied under quasi-static and dynamic loading conditions. Figure 7 is a schematic diagram of the experimental setup with the DMA to measure the mechanical properties of the TM.

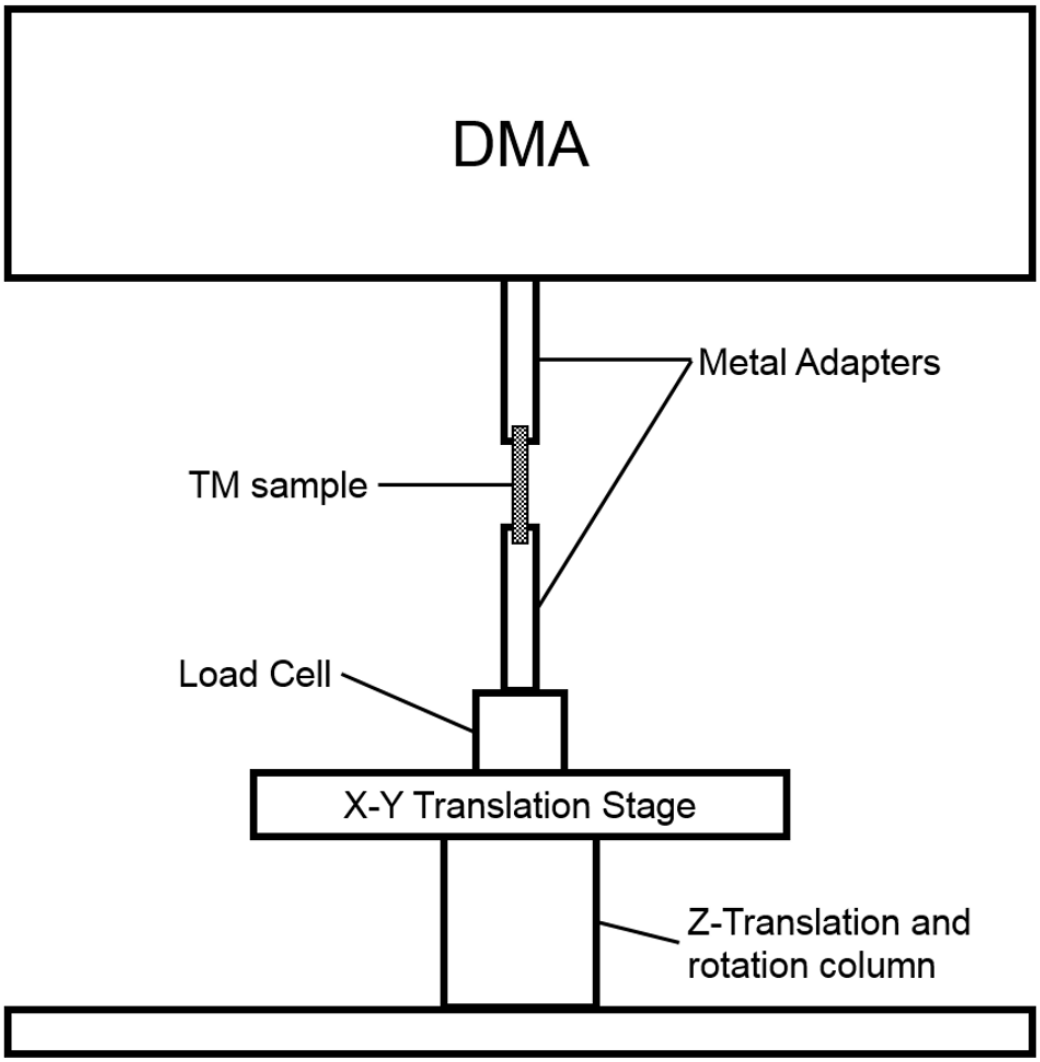

Figure 7. Schematic drawing of the DMA experimental setup.

The TM strip specimen was placed inside the DMA temperature-controlled chamber in the DMA. The bottom adapter was attached to a fixture, which was connected to the WMC-5-455, 5lb$_f$ load cell (Bose, MN) on an *x*, *y*, and *z*-axis

translational stage with *z*-axis rotation. The top adapter was attached to a fixture, which was connected the linear electric motor inside the DMA. A thermometer with a precision of ±1°C was placed at 2 cm behind the sample to monitor the temperature in the chamber. In the temperature change from 5°C to 37°C, there is no phase change (freezing) of fluid in tissue cells, and there is no denature of proteins. Thus, the structure of the soft tissue in this temperature range should not change [37,38]. During quasi-static, and low-frequency dynamic testing, the temperature was set to 25°C, but during frequency-temperature superposition testing, the temperature changed in this range. To maintain approximate physiological condition of the sample throughout the testing process, a damp saline cloth was applied to the medial surface of the TM between the individual tests and rest periods.

2.4 Quasi-Static Testing

2.4.1 Preconditioning

It is well known that the stabilized mechanical state of biological soft tissue can be reached through preconditioning [1]. In this study, preconditioning was achieved by conducting three loading and unloading cycles in the DMA. The specimens were elongated at a frequency of 0.05 Hz with a longitudinal stretch ratio of 10%. Three cycles of load-displacement curves for one TM was recorded in DMA. The hysteresis and peak load decreased with each successive cycle, and a steady state was observed at the second cycle.

2.4.2 Uniaxial Tension

After preconditioning, the sample was tested at 0.01 Hz with the elongation length was set to 15% of the samples original length. To compare results to the previous study by Cheng et. al, the stretch ratio for this test was kept the same, but the strain rate was approximately 80% slower [7].

2.4.3 Stress Relaxation

The stress relaxation test was performed to further develop current understanding of the mechanical properties of the baboon TM. Following previously established methodologies, a step function of elongation was applied to the sample at the beginning ($t = 0$) with a strain rate of 1.8 mm/s to an elongation length of 15% of the original length [7]. The stresses corresponding to the initial stress response σ_0 at $t = 0$ and the relaxed stress $\sigma(t)$ were recorded for a maximum of 200 s, during which the specimens were either relatively stable or fully relaxed at this point. After 200 seconds, the data recording software was stopped, and the sample was returned to its original unstressed state for dynamic testing.

2.4.4 Data Analysis for Quasi-Static Viscoelasticity

The experimental data under quasi-static loading measured from the DMA tests were processed to obtain: the stress-strain relationship, the normalized stress relaxation function $G(t)$, and the tangent modulus-stretch relationship. The TM's for all age groups were assumed to be isotropic, and determined to be a non-linear viscoelastic material based on observations from the load-displacement curves recorded during

preconditioning and uniaxial tension tests. For elasticity analysis, a hyperelastic material model was implemented for analyzing the data. The mechanical properties of biological materials can be analyzed by several non-linear material models, such as the Ogden, Mooney-Rivlin and Yeoh models. For studying rubber-like biological soft tissues, Sarma et al. showed that from the available models the Ogden model was the most valid and useful to explain the stress-strain behavior of smooth muscle tissue [39]. In literature, Ogden model was used to predict the behavior of several non-linear and viscoelastic biological tissues such as the skin, brain and the normal human TM [7,39-41]. In this study, the Ogden model was used to analyze the quasi-static experimental data of the baboon TM.

The Ogden model is generally expressed for elongation along a single axis as

$$\sigma = \frac{2\mu_1}{\alpha_1}\left[(1+\varepsilon)^{\alpha_1-1} - (1+\varepsilon)^{-(0.5\alpha_1+1)}\right] \quad (1)$$

where σ is the normal stress, ε is the strain, μ_1 is the initial shear modulus and α_1 is the incompressibility parameter [42]. In this study, the strain was converted to the stretch ratio, λ, which is defined as the deformed length to the original length for example,

$$\varepsilon = \frac{L}{L_0} \; and \; \lambda = \frac{L+L_0}{L_0} = \varepsilon + 1 \quad (2)$$

with this Eq. (1) becomes,

$$\sigma = \frac{2\mu_1}{\alpha_1}\left[(\lambda)^{\alpha_1-1} - (\lambda)^{-(0.5\alpha_1+1)}\right] \quad (3)$$

Differentiating Eq. (3) with respect to λ provides

$$\frac{d\sigma}{d\lambda} = \frac{2\mu_1}{\alpha_1}\left[(\alpha_1-1)\lambda^{\alpha_1-2} - \left(\frac{\alpha_1}{2}+1\right)\lambda^{-(0.5\alpha_1+2)}\right] \quad (4)$$

which gives the relationship between the tangent modulus $\frac{d\sigma}{d\lambda}$ and the stretch ratio λ.

The stress-strain loading curves measured during the uniaxial tension test were used to obtain the two material constants μ_1 and α_1, and were solved for by utilizing the curve fitting software in ANSYS Workbench (ANSYS, Inc., Canonsburg, PA). By substituting μ_1 and α_1 into Eq. (3) and Eq. (4), the constitutive equation of the TM in the Ogden form, and the tangent modulus with respect to stretch ratio were determined, respectively.

2.5 Dynamic Testing

The TM samples were subjected to small amplitudes with sinusoidal loading at different frequencies. The displacement *d* and force *F* were recorded as a function of time *t* for each frequency *f*,

$$d = d_o e^{i2\pi ft} \tag{8}$$

$$F = F_0 e^{i(2\pi ft + \delta)} \tag{9}$$

The complex modulus, *E**, at a single frequency was calculated as,

$$|E^*| = \frac{\sigma_0}{\varepsilon_0} = \frac{F_0/wh}{d_0/l} \tag{10}$$

$$E' = |E^*| \cos\delta \tag{11}$$

$$E'' = |E^*| \sin\delta \tag{12}$$

where *w*, *h*, and *l* were the width, thickness, and length of the specimen, respectively.

2.5.1 Low-Frequency Testing

Low-Frequency dynamic tests were performed on G1, G2, and G3 using a single temperature point at 25°C. The TM was tested at eight frequencies: 1, 2, 5, 10, 20, 40, and 80 Hz using a 50 Hz filter for 20 Hz and below. The displacement amplitude was

set to 15% strain of the sample's length. The specimen was given a rest period of 2 mins after each frequency point.

2.5.2 Frequency-Temperature Superposition (FTS)

The frequency-superposition method was performed on the adult baboon group. The FTS test used similar methods as low-frequency testing described in *2.5.1* except with a few additions. After the adult group was tested at 25°C the temperature was shifted to 5°C and finally to 37°C. For each temperature, the sample was tested at the same frequency points and displacement amplitude as low-frequency testing. The temperature of 37°C will be used as the reference temperature for the FTS principle.

The FTS principle was first reported in the 1950's, and has developed into a critical extrapolation technique when utilized for polymers, plastic, and composites [43,44]. The principle further developed to establish a simple relationship between temperature and frequency (or time) and their effects on polymers and viscoelastic materials at the molecular level [45]. Recently, the FTS principle has been used to determine the dynamic properties of the human TM in the auditory frequency range [13]. The curves of the complex modulus E^* obtained at relatively low temperatures with a reference temperature T_0 can be shifted along the frequency axis by a shift factor α_T to a higher frequency T. This concept can be expressed by the equation,

$$E^*(T_0, f) = E^*(T, f/\alpha_T) \tag{13}$$

where f is the frequency. The temperature's effect on the material's complex modulus can be quantified by the shift factor α_T. It is temperature-dependent and needs to obey the Arrhenius equation,

$$\ln \alpha_T = \frac{E_a}{R}\left(\frac{1}{T} - \frac{1}{T_0}\right) \quad (14)$$

where T and T_0 are the absolute temperature in Kelvin, E_a is the activation energy for the material, and R is the universal gas constant equal to 8.314 J/mol K [46].

The Williams-Landel-Ferry (WLF) equation is an additional widely used empirical equation for the FTS principle, which was first introduced by Williams et al.,

$$\log \alpha_T = \frac{c_1(T - T_g)}{c_2 + T - T_g} \quad (15)$$

where c_1 and c_2 are empirical constants and T_g is the glass transition temperature [44]. The glass transition temperature is defined as the temperature below which the polymer chain backbone configuration rearrangement stops [47]. Combining the Eqs. (14) and (15) yields the relationship between the activation energy E_a and the empirical constant c_1 and c_2,

$$E_a = 2.303R\frac{c_1 c_2 T^2}{(c_2 + T - T_g)^2} \quad (16)$$

Following previous methods, the procedure to determine the dynamic properties of the adult baboon TM in the auditory frequency range was used [13]. First, the complex modulus in terms of the storage E' and loss E'' modulus was obtained at three different temperatures 5, 25, and 37°C, and plotted together as functions of frequency on a logarithmic scale. Second, the complex modulus curves associated with the lower temperatures were shifted along the frequency axis towards higher frequencies. The commonly called "Master Curve" was formed with a reference temperature at 37°C when the complex modulus curves were adjacent to each other, and was then used to predict the complex modulus at the higher frequency range. Finally, Eqs. (13) and (14) were used to calculate the shift factor α_T and the activation energy E_a. There are three

requirements for creating the Master Curve that must be met for the FTS principle to hold: (1) perfect matching of the curve shapes at adjacent range regions, (2) same shift factor value for all viscoelastic parameters, and (3) the shift factor must obey the Arrhenius or the WLF equation. The first requirement was met when the percent difference between the complex modulus in adjacent regions was less than 10%, and the remaining requirements were checked through careful observation and satisfied [13].

2.6 Failure Testing

To determine the age effect on the mechanical strength of the baboon TMs, failure testing was performed on all specimens. Following previous methodologies, the strain rate was set to 0.1 mm/s [7]. During the failure process the TM strip was observed, and the location of failure was observed.

2.7 Scanning Electron Microscopy

To better understand the microstructural composition of the baboon TM, scanning electron microscopy (SEM) imaging was performed for the adult TM group. For SEM preparation the temporal bone surrounding, the TM was removed such that the entirety of the TM could be easily viewable from either the medial or lateral side and still maintain the tension on the TM. Following previous methodologies, the TM specimen was fixed in paraformaldehyde for 24 hours. The specimens were dehydrated in ethanol in increasing concentrations from 30% to 100% allowing the sample to remain in each solution once for 15 min and three times at 100% for 10 min. Sample was dried using Hexamethyldisilizane solution, and sputter coated with gold palladium.

To reduce charging the surrounding temporal bone was coated using silver paste. The prepared samples were examined with electron microscopes (NEON 40 EsB, Zeiss, Oberkochen, Germany) (JSM-840, JEOL Ltd., Tokyo, Japan) the operating voltage was set as 5 V, and the working distance was set to 5.7 mm [48]. SEM work was performed in the Samuel Roberts Noble Microscopy Laboratory at the University of Oklahoma.

2.8 Statistical Analysis

To determine any significant difference in the mechanical properties from young to adult baboon TM statistical analysis was performed on the experimental data obtained from the quasi-static uniaxial, relaxation, and low-frequency dynamic testing. For each type of test the TMs that were less than 1 (G1), between 1 and 3 (G2), between 3 and 5 (G3), and older than 5 years of age (G4) were used for the analysis. A one-way analysis of variance (ANOVA) with an alpha level of 0.1 was used to determine significance. For the analysis, the null hypothesis set was that the sample mean for G1, G2, G3, and G4 were equal, and the hypothesis was that there was at least one inequality. Additionally, six group pairings were created: G1 vs G2, G1 vs G3, G1 vs G4, G2 vs G3, G2 vs G4, and G3 vs G4. If ANOVA detected significance between groups the Tukey-Kraemer analysis was used to determine where that significance was located, and a “Yes” or “No” was used to denote significant difference between groups.

Chapter 3: Results

3.1 Quasi-Static Experimental Data

The experiments were performed on four groups of baboons with age ranges of less than 1, 1 to 3, 3 to 5, and older 5 years of age. The baboon groups were designated as G1, G2, G3 and G4, where G1 is the youngest and G4 is the oldest. In G1, there were a total of 7 samples with a mean age, length, width, and thickness of 67 ± 26 days, 5.64 ± 0.39 mm, 1.80 ± 0.28 mm, and 0.025 ± 0.004 mm, respectively. In G2, there were a total of 8 samples with an average age, length, width, and thickness of 2.3 ± 0.9 years, 5.76 ± 0.86 mm, 1.80 ± 0.24 mm, and 0.028 ± 0.010 mm. In G3, there were a total of 8 samples with an average age, length, width, and thickness of 4.2 ± 0.5 years, 5.83 ± 0.69 mm, 1.84 ± 0.23 mm, and 0.023 ± 0.003 mm, respectively. In G4, there were a total of 5 samples with an average age, length, width, and thickness of 10.9 ± 4.0 years, 5.46 ± 0.68 mm, 1.70 ± 0.32 mm, and 0.025 ± 0.003 mm.

3.1.1 Preconditioning

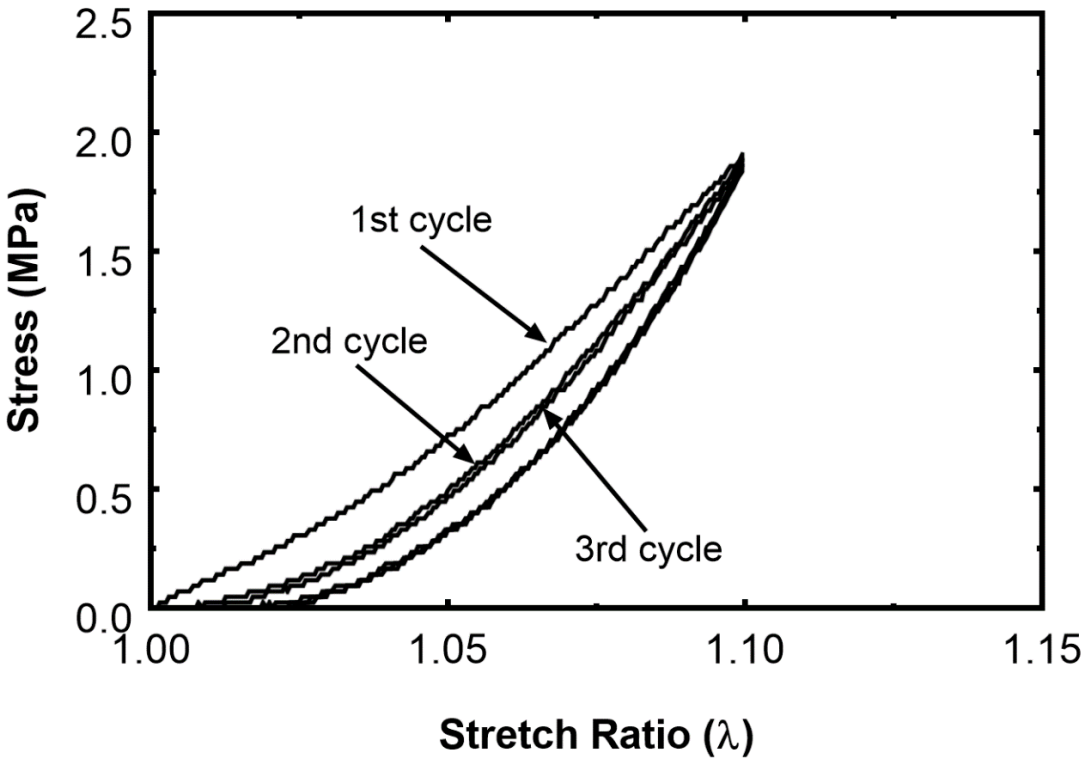

Figure 8. Preconditioning figure of a typical sample. Shown are the first, second, and third cylces.

Three cycles of loading and unloading were recorded by the DMA and load-displacement curves were converted into stress-stretch ratio curves shown in Figure 8, the first, second, and third cycle are indicated by the labels with arrows. The unloading curve was always below the loading curve, and the sample reached a sampled state after the second cycle.

3.1.2 Uniaxial Tension

Figure 9 shows the stress-stretch ratio relationship of 7 TM specimens that the age range was 30 to 90 days during the uniaxial tensile test. All samples were stretched to a stretch ratio of 1.15 or 15% elongation. The maximum and minimum stresses occurred for sample 17-1R and 16-9R with a stress of 2.10 and 0.90 MPa. Figure 10 gives the stress stretch ratio relationship of 8 TM specimens that the age range was 1 to 3 years during the uniaxial tensile test. All samples were stretched to a stretch ratio of 1.15, except for 15-14L which was stretched to 1.14. The maximum and minimum stresses occurred for sample 16-4LP and 16-7L with a stress of 1.50 and 0.79 MPa. Figure 11 shows the stress stretch ratio relationship of 8 TM specimens that the age range was 3 to 5 years during the uniaxial tensile test. All samples were stretched to a stretch ratio of 1.15. The maximum and minimum stresses occurred for sample 17-10R and 17-2L with a stress of 1.50 and 0.76 MPa. Figure 12 shows the stress stretch ratio relationship of 5 TM specimens that the age range was older than 5 years during the uniaxial tensile test. All samples were stretched to a stretch ratio of 1.15. The maximum and minimum stresses occurred for sample 17-12L and 17-16L with a stress of 1.04 and 0.65 MPa.

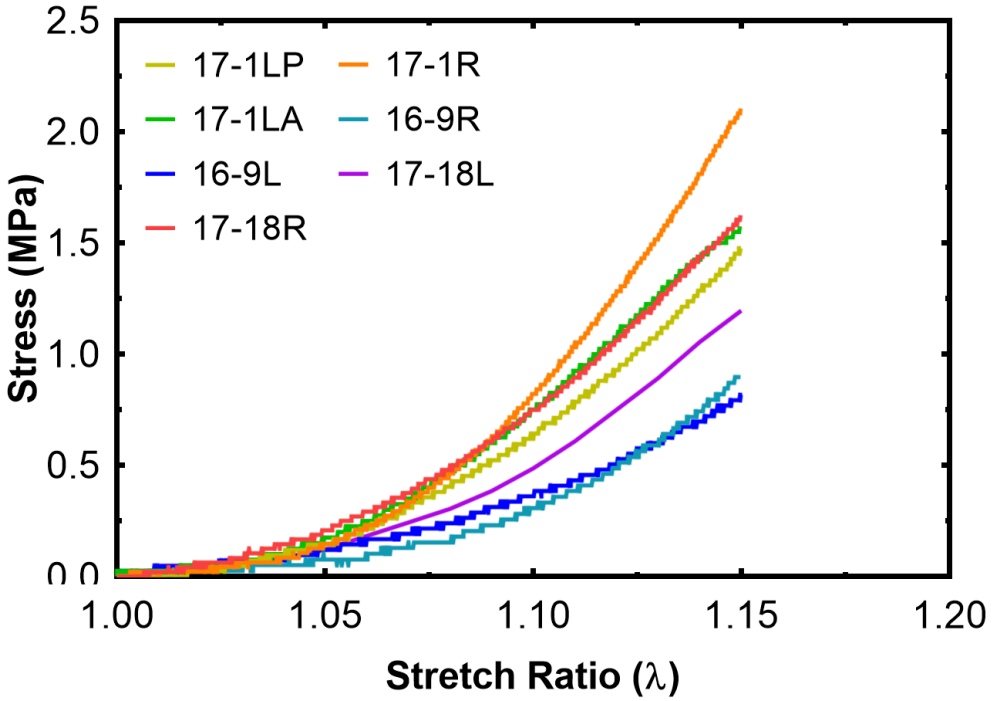

Figure 9. Individual stress and stretch ratio curves of G1 with 7 samples.

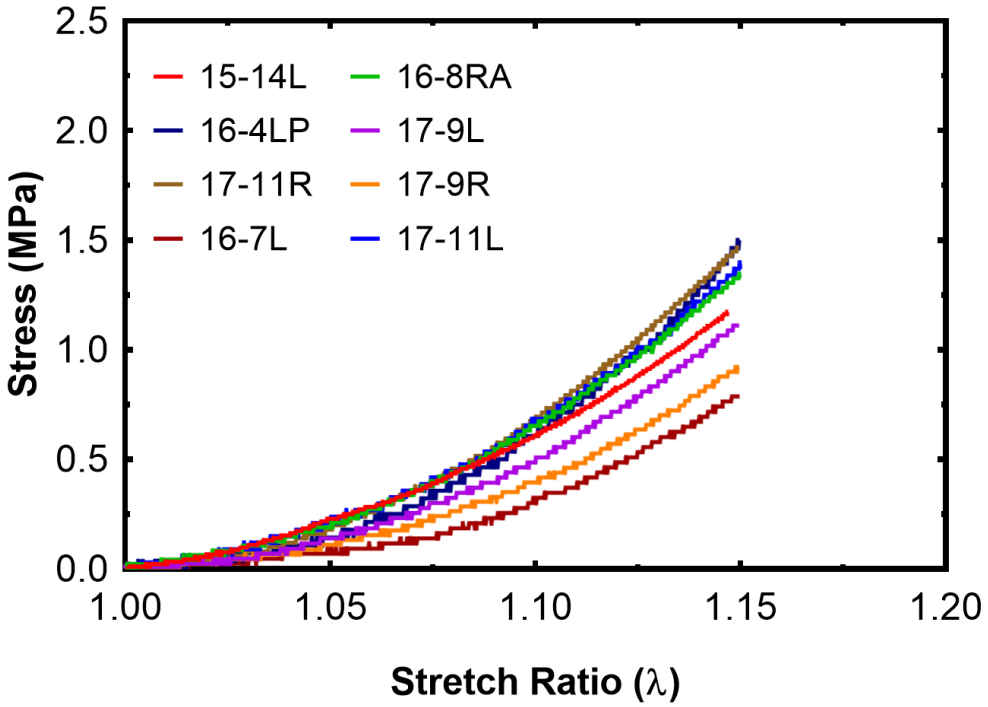

Figure 10. Individual stress and stretch ratio of G2 with 8 specimens.

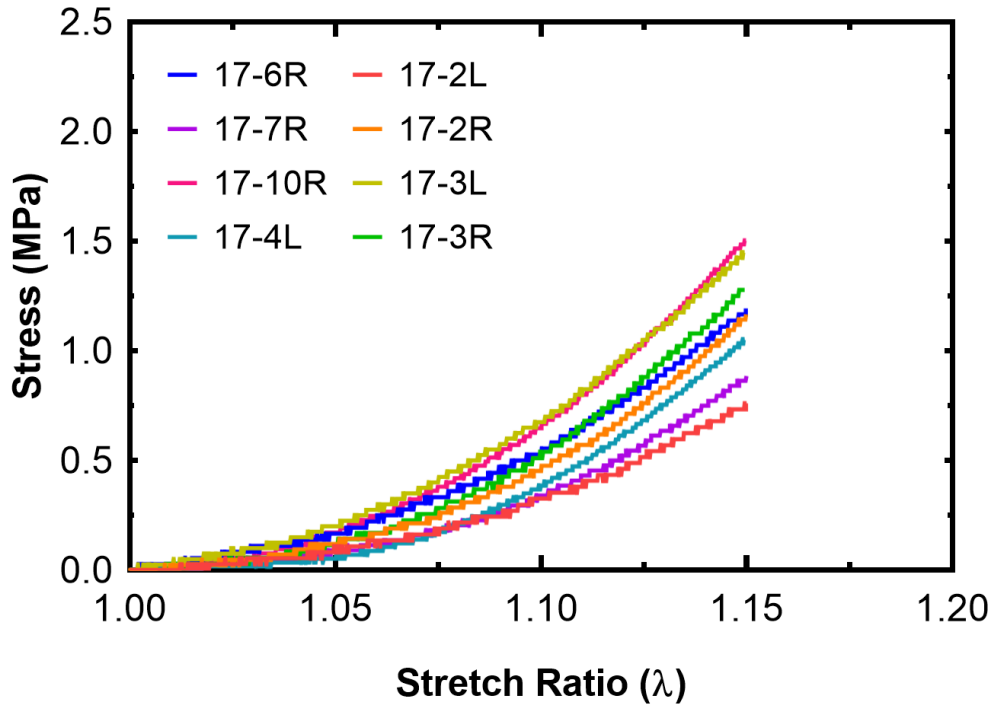

Figure 11. Individual stress and stretch ratio curves for G3 with 8 specimens.

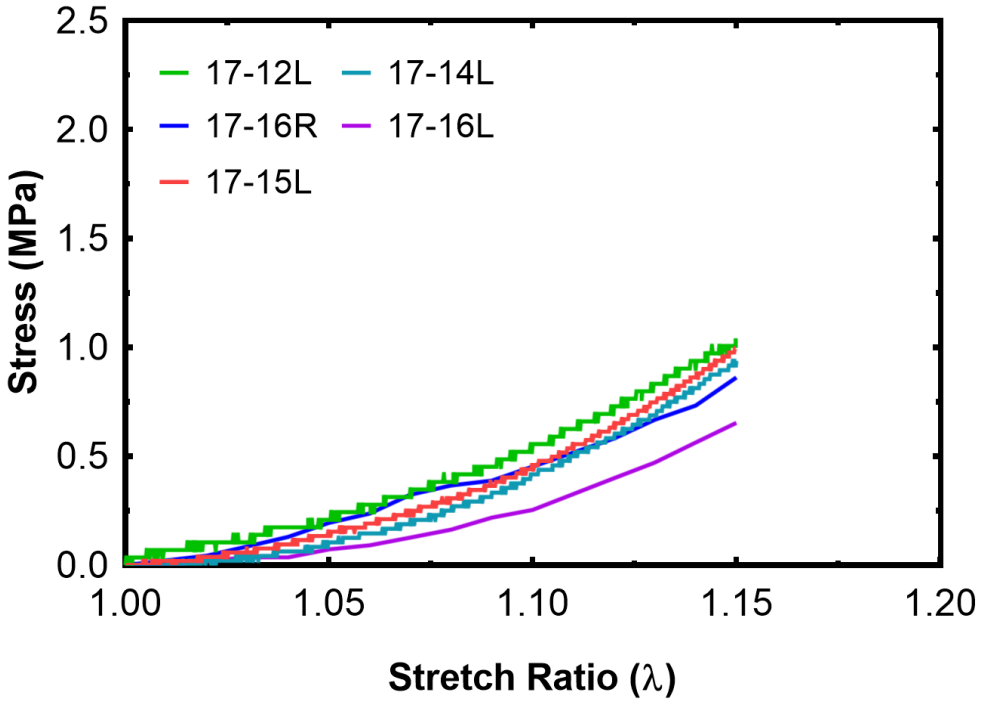

Figure 12. Individual stress and stretch ratio curves for G4 with 5 specimens.

3.1.3 Relaxation

For the following figures, the y-axis is the normalized stress relaxation G(t), and is defined as the ratio between the $\sigma(t)$ at time t and the initial stress at σ_0.

Figure 13 gives the stress relaxation of 5 TM samples with an age less than 1 year old. At 200 s the samples that relaxed the least and most were 17-18R and 17-1LA that relaxed to 18% and 26% of the maximum stress. Figure 14 gives the stress relaxation of 4 TM samples with an age between 1 and 3 years old. At 200 s the samples that relaxed the least and most were 17-11L and 17-9R that relaxed to 18% and 25% of the maximum stress. Figure 15 gives the stress relaxation of 8 TM samples with an age between 3 and 5 years old. At 200 s the samples that relaxed the least and most were 17-3L and 17-7R that relaxed to 22% and 36% of the maximum stress. Figure 16 gives the stress relaxation of 5 TM samples with an age more than 5 years old. At 200 s the samples that relaxed the least and most were 17-15L and 17-14L that relaxed to 21% and 29% of the maximum stress.

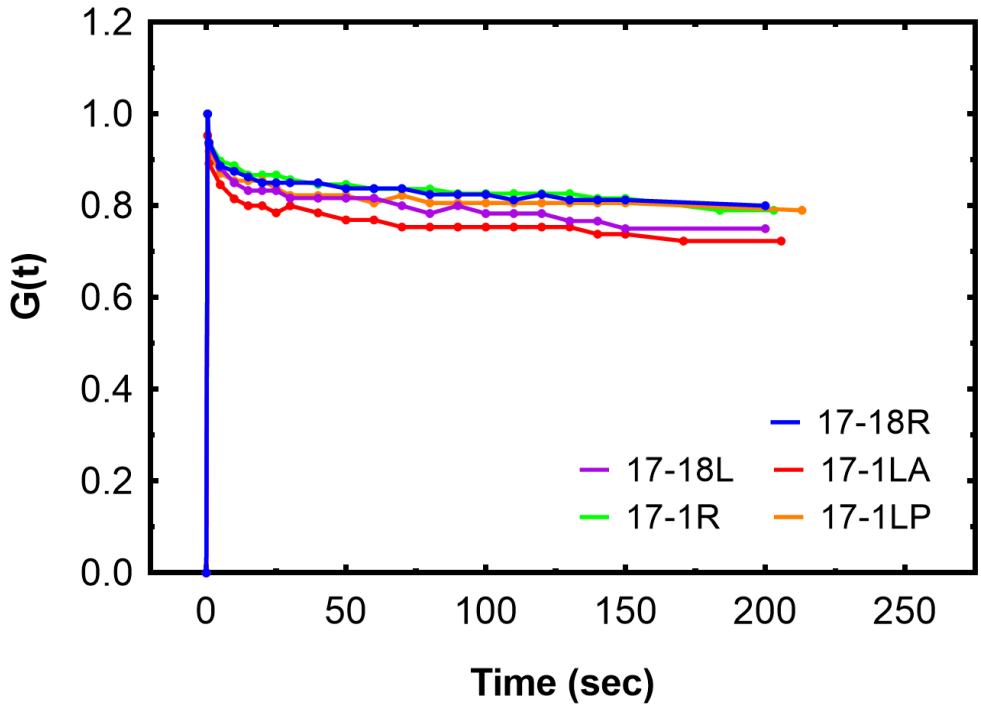

Figure 13. Stress relaxation for G1.

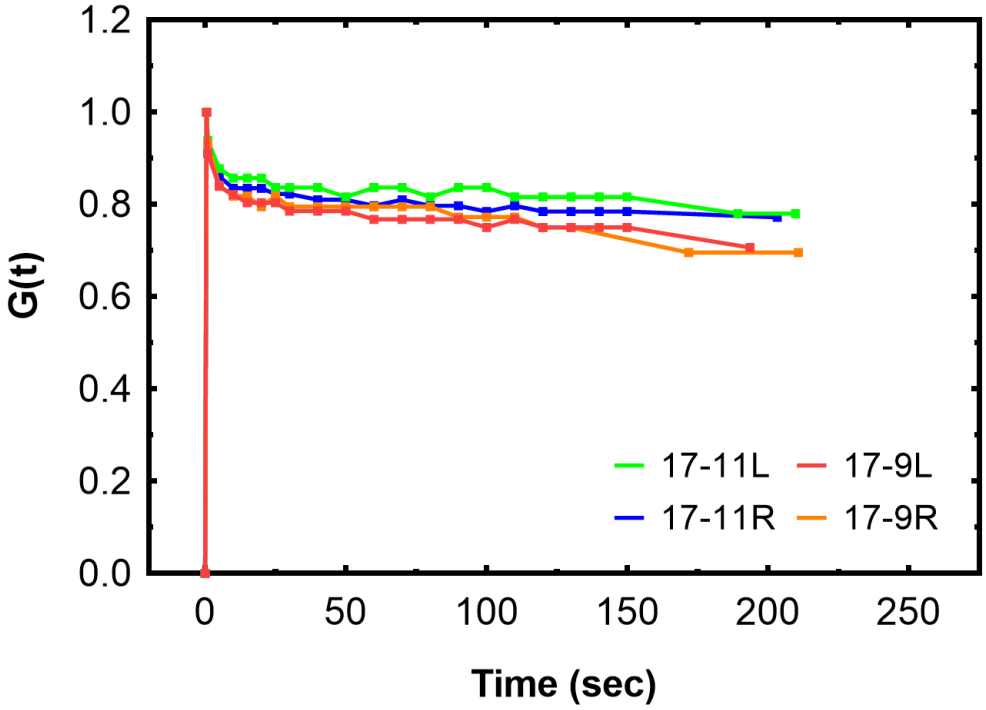

Figure 14. Stress relaxation for G2.

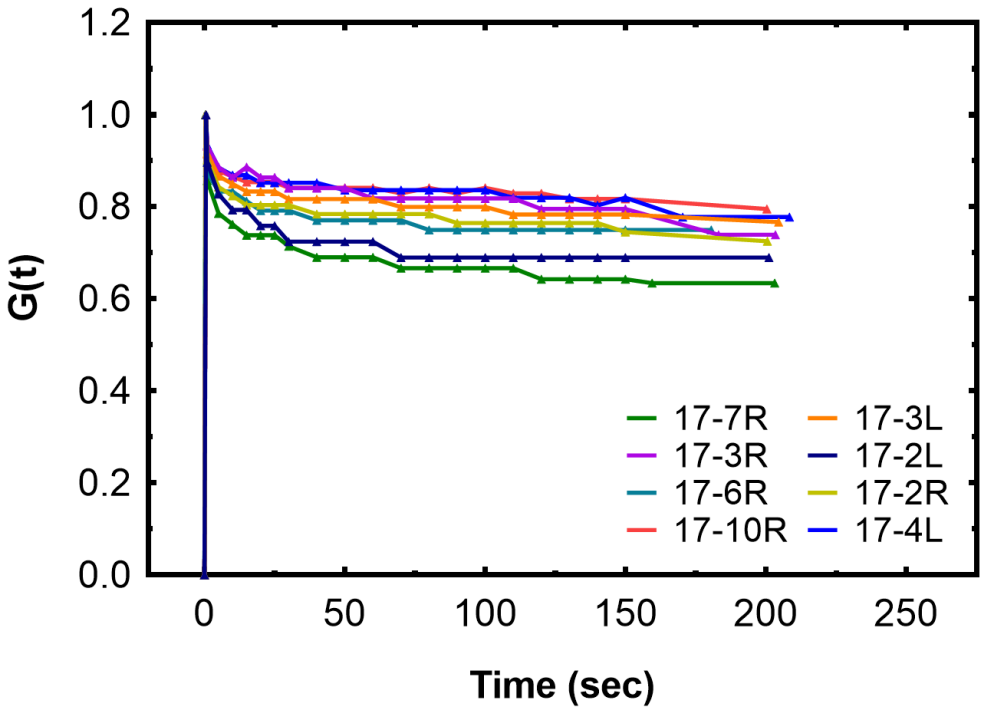

Figure 15. Stress relaxation for G3.

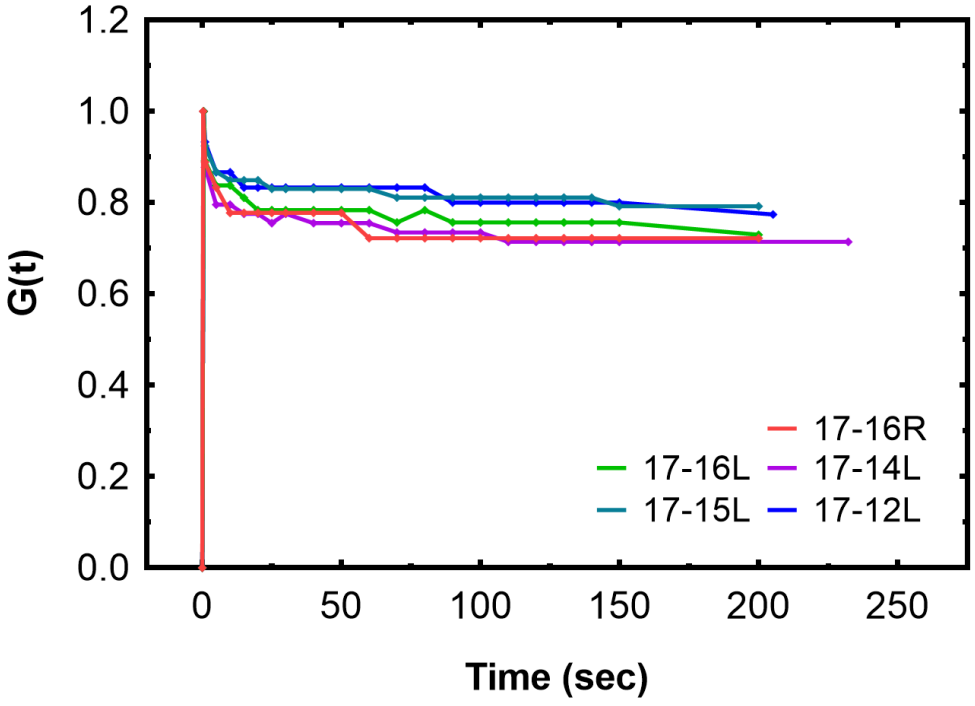

Figure 16. Stress relaxation for G4.

3.2 Dynamic Experimental Data

The direct measurement of the complex modulus was performed on four groups of baboons with age ranges of less than 1, 1 to 3, 3 to 5, and older 5 years of age, which are the same as the age groups mentioned in the static findings. Each group was tested in the low frequency range of 1 to 80 Hz at 25°C. However, the adult group was additionally tested at the temperatures of 5° and 37°C following the procedure described in section 2.5.2 Frequency-Temperature Superposition.

3.2.1 Low-Frequency

For G1 a total of 7 samples were tested with an average and standard deviation for the length 5.64 ± 0.39 mm, width 1.80 ± 0.28 mm, and thickness 0.025 ± 0.004 mm.

Figure 17 shows the storage modulus for the 7 samples in G1 the storage modulus is flat from 1 to 10 Hz, and monotonic increasing from 20 to 80 Hz. The maximum and minimum storage modulus at 1 Hz is 19.26 and 8.82 MPa for samples 17-1R and 16-9L. At 80 Hz the maximum is 28.01 MPa for 17-1LA and the minimum is 15.22 MPa for 17-18L. Figure 18 shows the loss modulus for the 7 samples in G1 the loss modulus is flat from 1 to 10 Hz, and monotonic increasing from 20 to 80 Hz. The maximum and minimum loss modulus at 1 Hz is 2.48 and 1.14 MPa for samples 17-1R and 16-9L. At 80 Hz the maximum is 2.33 MPa for 17-1R and the minimum is 0.99 MPa for 16-9R.

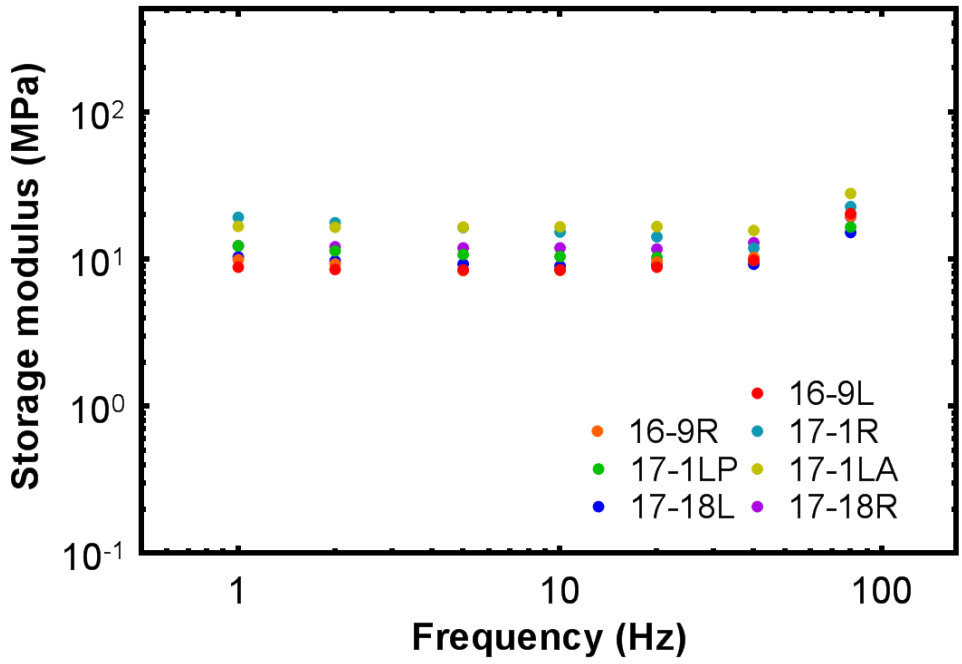

Figure 17. Direct dynamic measurement of the storage modulus in low frequency for G1.

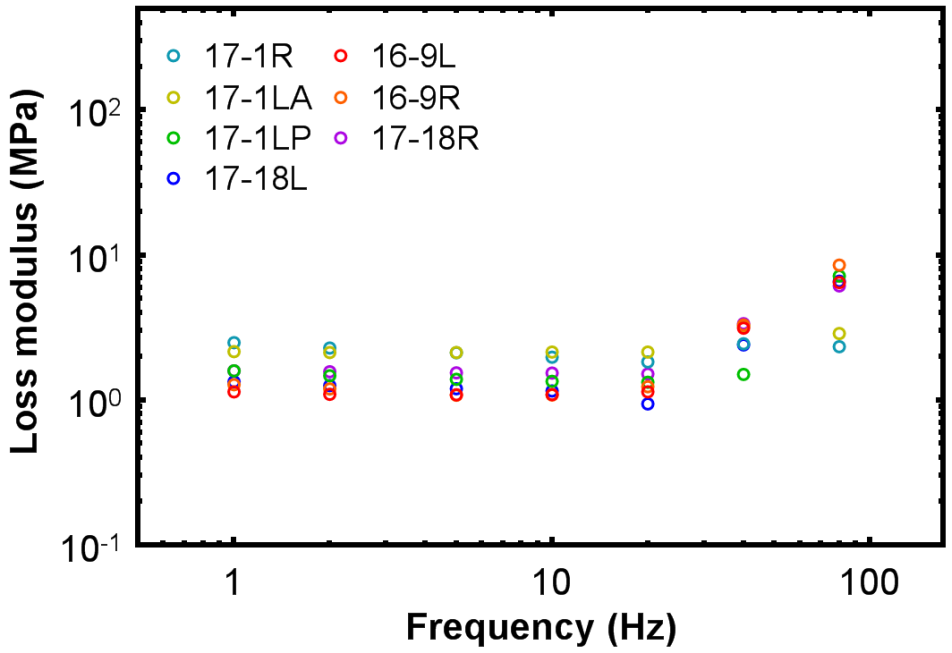

Figure 18. Direct dynamic measurement of the loss modulus in low frequency for G1.

For G2 a total of 9 samples were tested with an average and standard deviation for the length 5.94 ± 0.48 mm, width 1.82 ± 0.23 mm, and thickness of 0.0242 ± 0.004 mm.

Figure 19 shows the storage modulus for the 9 samples in G2 the storage modulus is flat from 1 to 10 Hz, and monotonic increasing from 20 to 80 Hz. The maximum and minimum storage modulus at 1 Hz is 15.80 and 6.44 MPa for samples 16-3RP and 16-7L. At 80 Hz the maximum is 29.09 MPa for 16-3RP and the minimum is 13.64 MPa for 17-9R. Figure 20 shows the loss modulus for the 9 samples in G2 the loss modulus is flat from 1 to 10 Hz, and monotonic increasing from 20 to 80 Hz. The maximum and minimum loss modulus at 1 Hz is 2.04 and 0.83 MPa for samples 16-3RP and 16-7L. At 80 Hz the maximum is 11.09 MPa for 17-11L and the minimum is 1.99 MPa for 16-8RA.

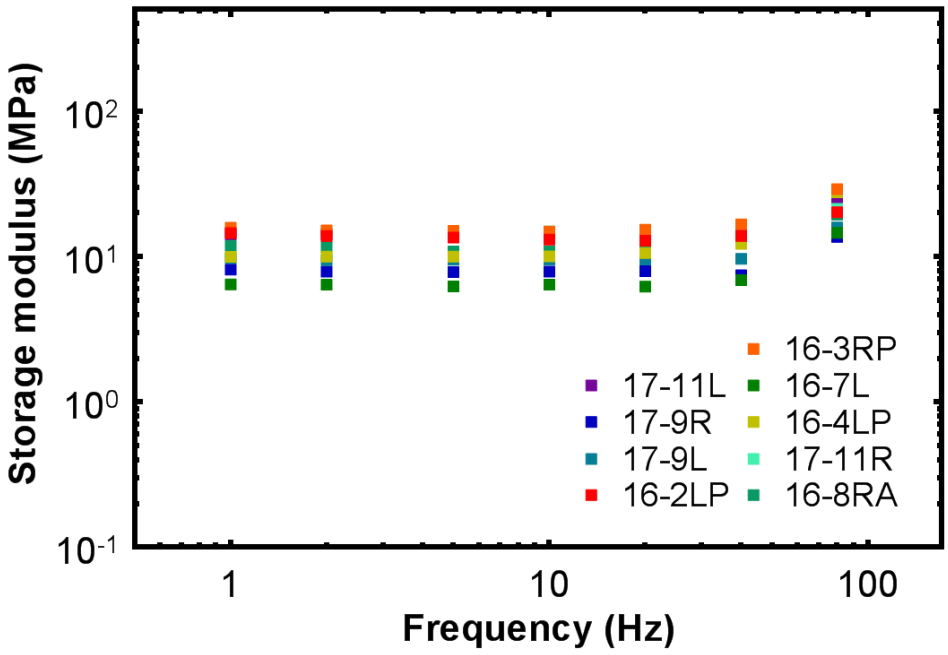

Figure 19. Direct dynamic measurement of the storage modulus in low frequency for G2.

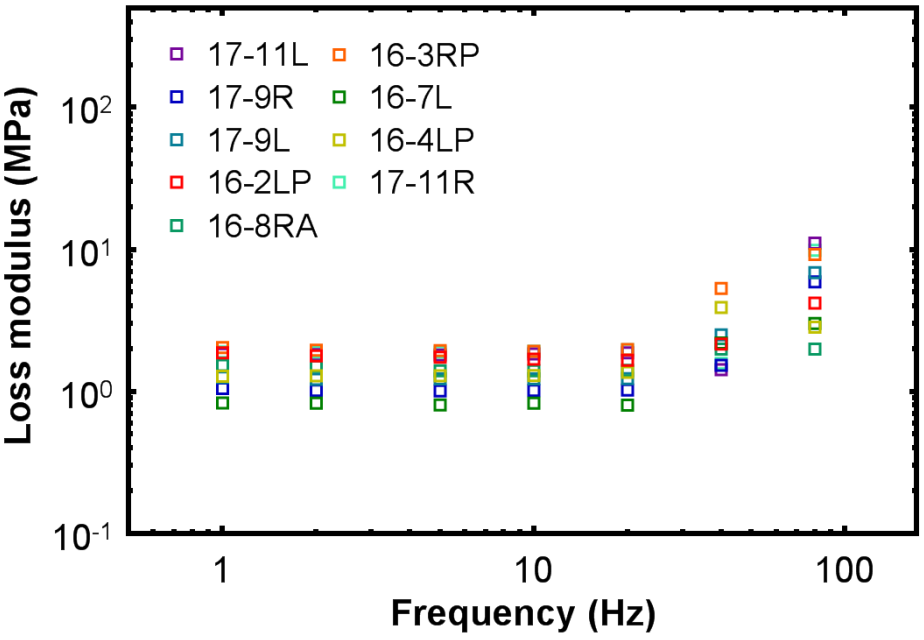

Figure 20. Direct dynamic measurement of the loss modulus in low frequency for G2.

For G3 a total of 7 samples were tested with an average and standard deviation length 6.03 ± 0.41 mm, width 1.81 ± 0.24 mm, and thickness of 0.024 ± 0.003 mm.

Figure 21 shows the storage modulus for the 7 samples in G3 the storage modulus is flat from 1 to 20 Hz, and monotonic increasing from 40 to 80 Hz. The maximum and minimum storage modulus at 1 Hz is 12.98 and 8.11 MPa for samples 17-4L and 17-2L. At 80 Hz the maximum is 21.39 MPa 17-2R and the minimum is 13.41 MPa for 17-2L. Figure 22 shows the loss modulus for the 7 samples in G3 the loss modulus is flat from 1 to 10 Hz, and monotonic increasing from 20 to 80 Hz. The maximum and minimum loss modulus at 1 Hz is 1.63 and 1.00 MPa for samples 17-10R and 17-3R. At 80 Hz the maximum is 8.73 MPa for 17-6R and the minimum is 2.17 MPa for 17-3L.

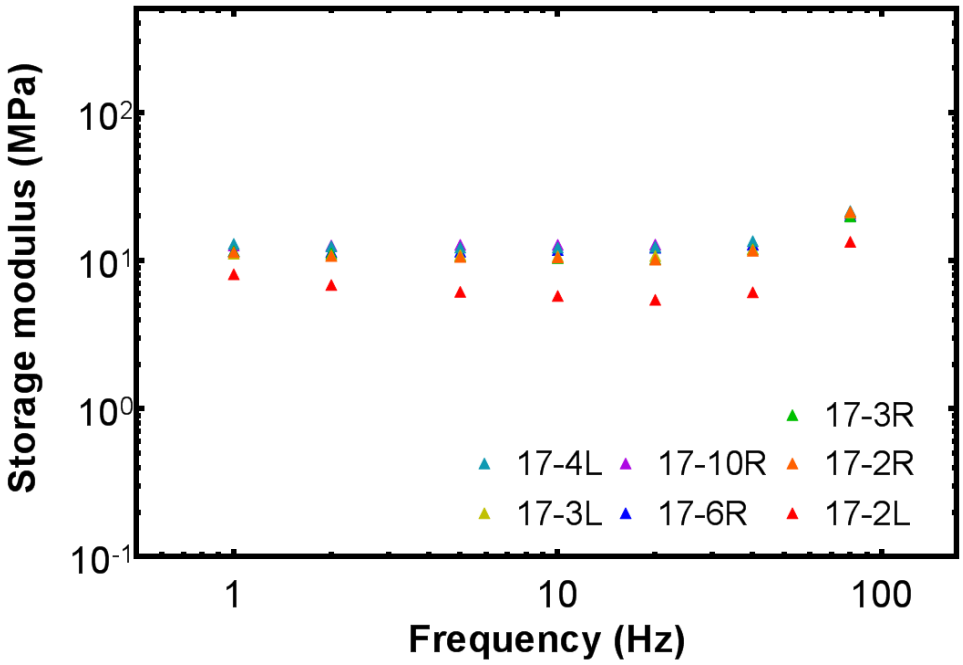

Figure 21. Direct dynamic measurement of the storage modulus in low frequency for G3.

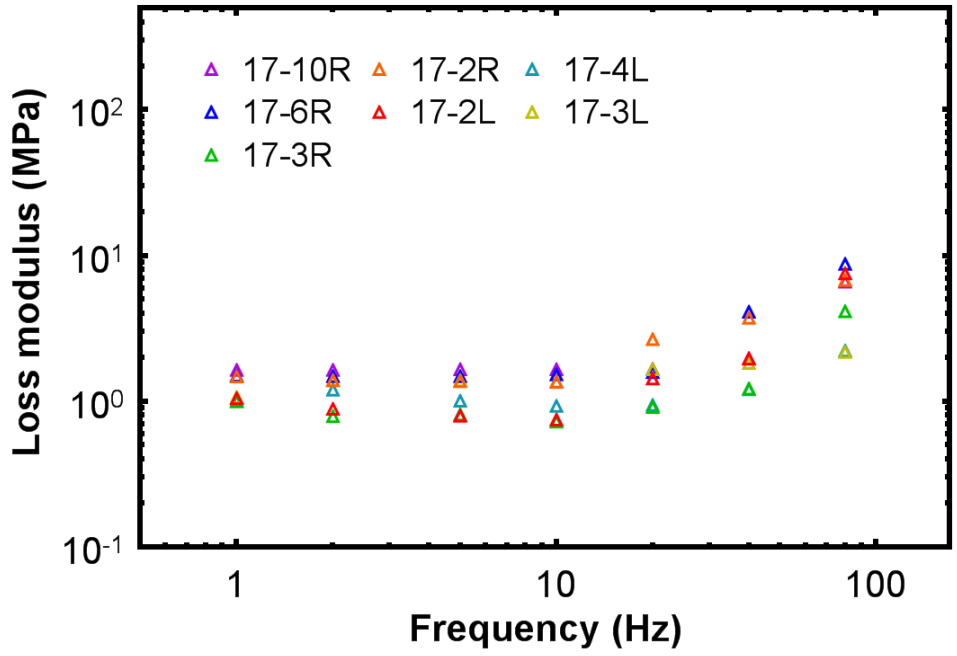

Figure 22. Direct dynamic measurement of the loss modulus in low frequency for G3.

For G4 a total of 8 samples were tested with an average and standard deviation for the length 5.68 ± 0.70 mm, width 1.74 ± 0.28 mm, and thickness of 0.024 ± 0.003 mm.

Figure 23 shows the storage modulus for the 8 samples in G4 the storage modulus is flat from 1 to 20 Hz, and monotonic increasing from 40 to 80 Hz. The maximum and minimum storage modulus at 1 Hz is 14.33 and 4.81 MPa for samples 17-12R and 17-16R. At 80 Hz the maximum is 26.01 MPa for 17-14R and the minimum is 10.94 MPa123 for 17-16R. Figure 24 shows the loss modulus for the 8 samples in G4 the loss modulus has a small peak around 2 Hz, and is followed with an increase from 20 to 80 Hz. The maximum and minimum loss modulus at 1 Hz is 0.57 and 0.36 MPa for samples 17-15L and 17-12L. At 80 Hz the maximum is 10.37 MPa for 17-12L and the minimum is 1.58 MPa for 17-15L.

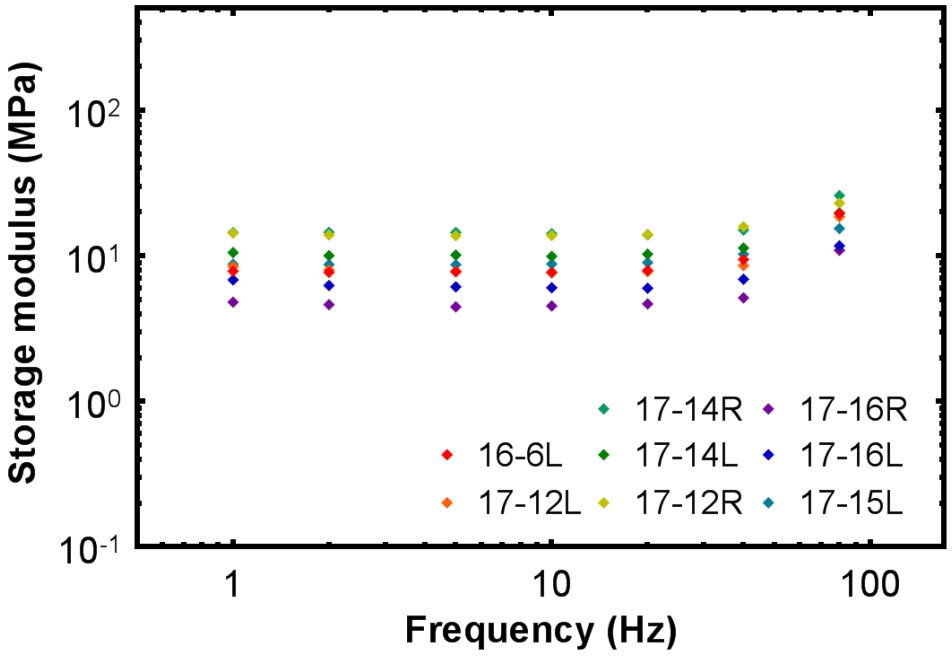

Figure 23. Direct dynamic measurement of the storage modulus in low frequency for G4.

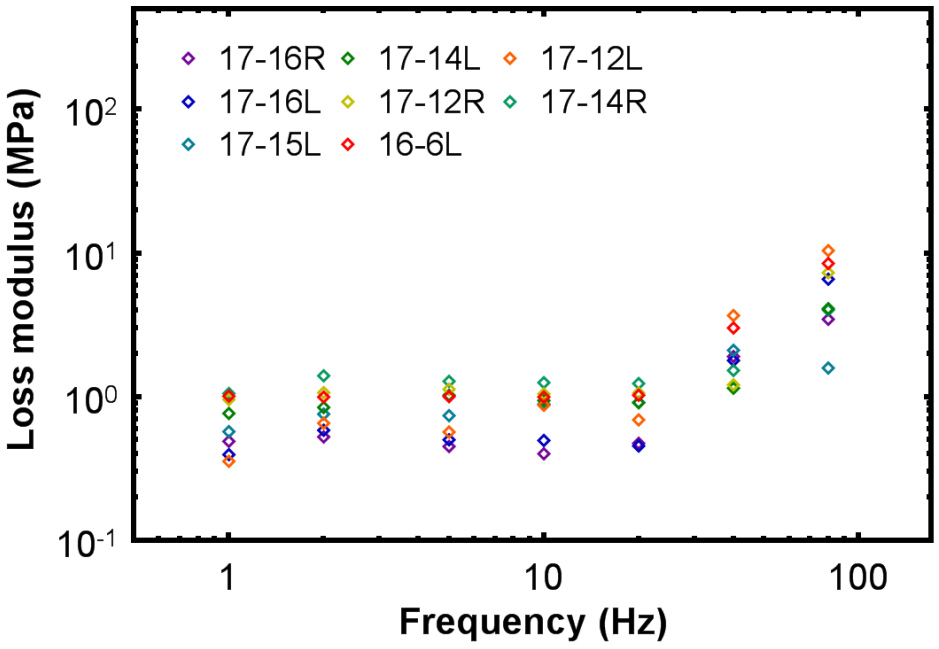

Figure 24. Direct dynamic measurement of the loss modulus in low frequency for G4.

3.2.2 Frequency-Temperature Superposition

The FTS principle was performed on only the adult baboon group where each sample was older than 5 years of age, and the maximum age was 15 years old. Figure 25 and Figure 26 are two typical samples showing the storage and loss modulus for the temperature 5°C, 25°C, and 37°C both before and after applying the shift factor.

As seen by the two examples (17-3L and 17-12R) the storage and loss modulus increased with increasing frequency or with decreasing temperature. Following the FTS principle mentioned in the "Frequency-Temperature Superposition" section the lower temperatures were shifted to a higher frequency range and the master curve was created. The complex modulus curves are well matched in the adjacent regions with a percent difference of less than 6%. Therefore, the first requirement of the FTS principle is satisfied, and the shift factors for the storage and loss modulus for each specimen is the same satisfying the requirement. For 17-3L, the storage modulus has a slight increase from 1 Hz to 8000 Hz increasing from 8.86 to 14.13 MPa, and 17-12R has a slight increase from 1 Hz to 8000 Hz increasing from 13.44 to 17.66 MPa. The loss modulus for 17-3L is 0.56 MPa at 1 Hz and is followed by a quick rise to 20 Hz where it is relatively stable until 2000 Hz where it increases from 1.59 MPa to 3.66 MPa at 8000 Hz. For 17-12R the loss modulus is relatively flat with a slight increase from 0.85 MPa at 1 Hz to 1000 Hz where it increases from 1.10 MPa to 4.57 MPa at 8000 Hz.

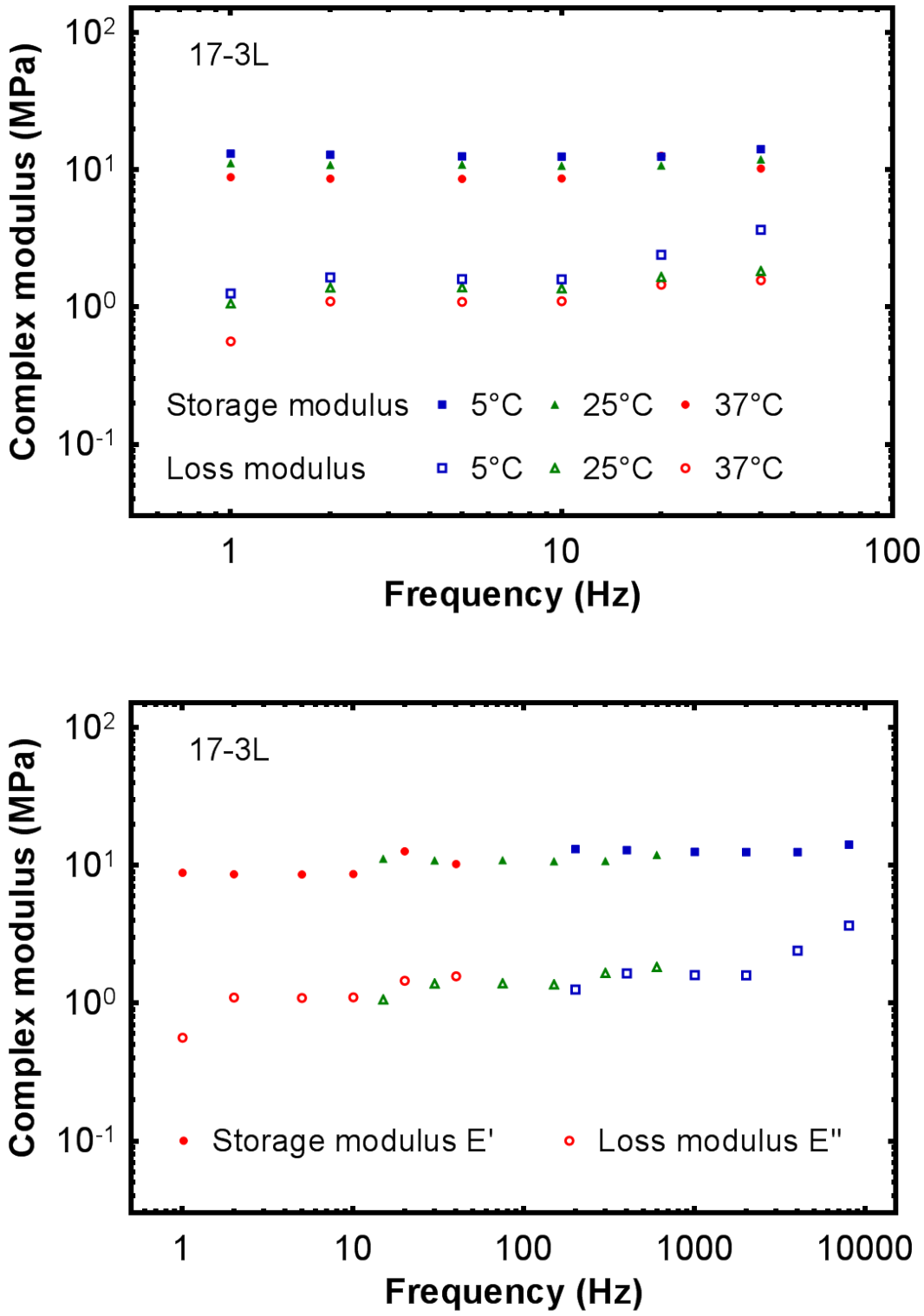

Figure 25. 17-3L represents a typical direct measurement of storage and loss modulus at each temperature before shifting lower temperatures to higher frequency.

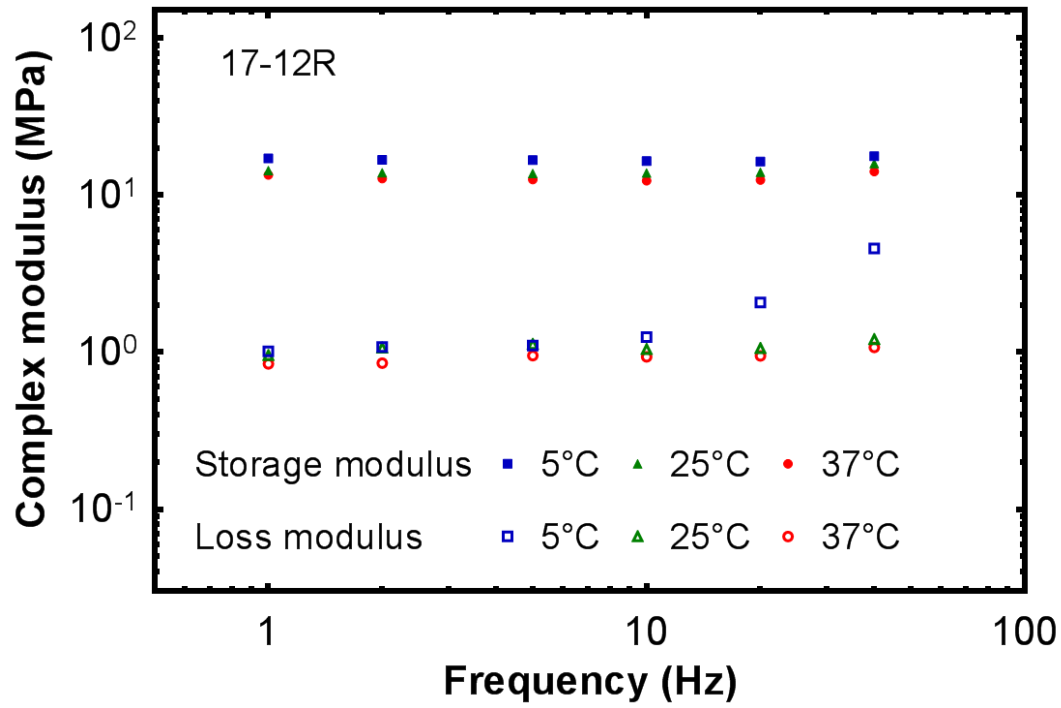

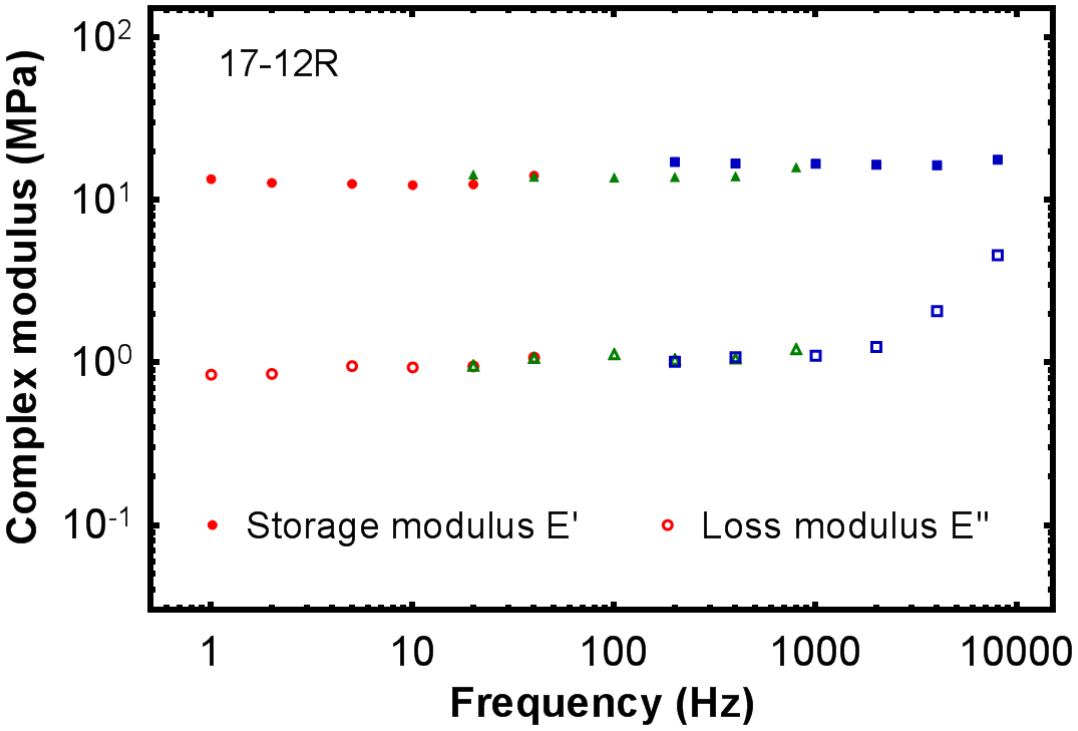

Figure 26. 17-12R gives an additional example of the direct measurement of storage and loss modulus at each temperature before shifting lower temperatures to higher frequency.

Figure 27 gives the storage modulus for 8 samples of adult baboons. For all samples the storage modulus has a small increase across the entire frequency range. At 1 Hz the maximum and minimum storage modulus is 13.44 MPa for 17-12R and 4.09 MPa for 17-16R. At 8000 Hz the maximum and minimum storage modulus is 17.66 MPa for 17-12R and 7.56 MPa for 17-16R. Figure 28 gives the loss modulus for 8 samples of adult baboons. Each sample features relatively the same pattern of the loss modulus initially having a sharp increase from 1 to 5 Hz, then a slight increase from 10 to 1000 Hz where it rapidly increases to its maximum at 8000 Hz. At 1 Hz the maximum and minimum storage modulus is 0.85 MPa for 17-12R and 0.27 MPa for 17-16R. At 8000 Hz the maximum and minimum storage modulus is 4.57 MPa for 17-12R and 0.77 MPa for 17-16R. The shift factors for all adult baboon samples are summarized in the first two columns of Table 13. The average value for the shift factor from 25°C to 37°C was 15.6 ± 5.0 and the average value for the shift factor from 5°C to 37°C was 193.8 ± 17.7. Using Eq. 14 the average activation energy was 117.83 ± 2.78 kJ/mol. The maximum frequency achieved was 8000 Hz for all specimens. The average length, width, and thickness were 5.68 ± 0.70 mm, 1.74 ± 0.28 mm, and 0.024 ± 0.003 mm, respectively.

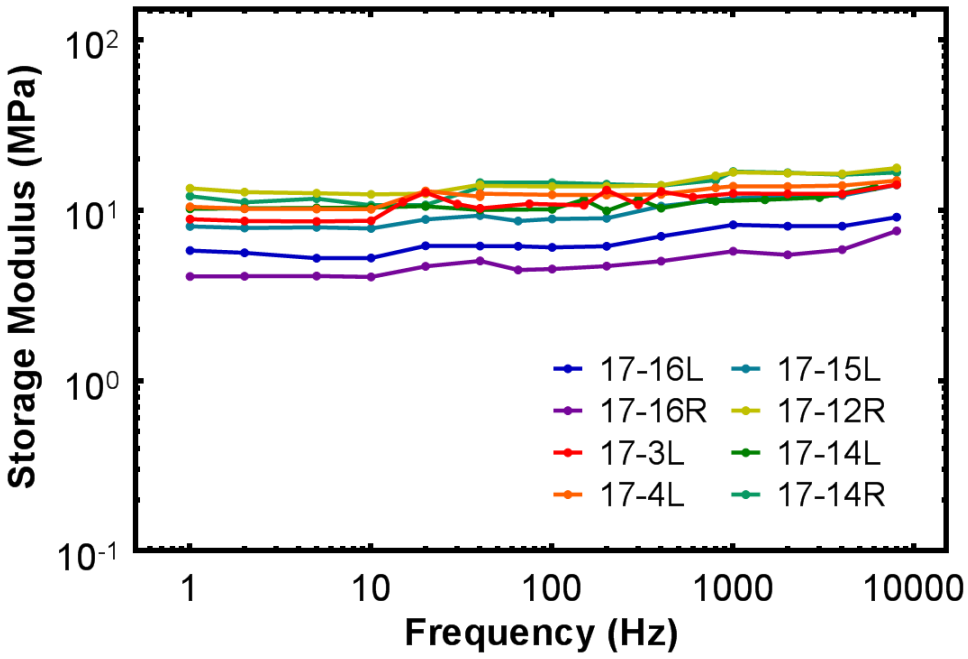

Figure 27. Direct dynamic measurement of the storage modulus in high frequency using FTS for adult baboons.

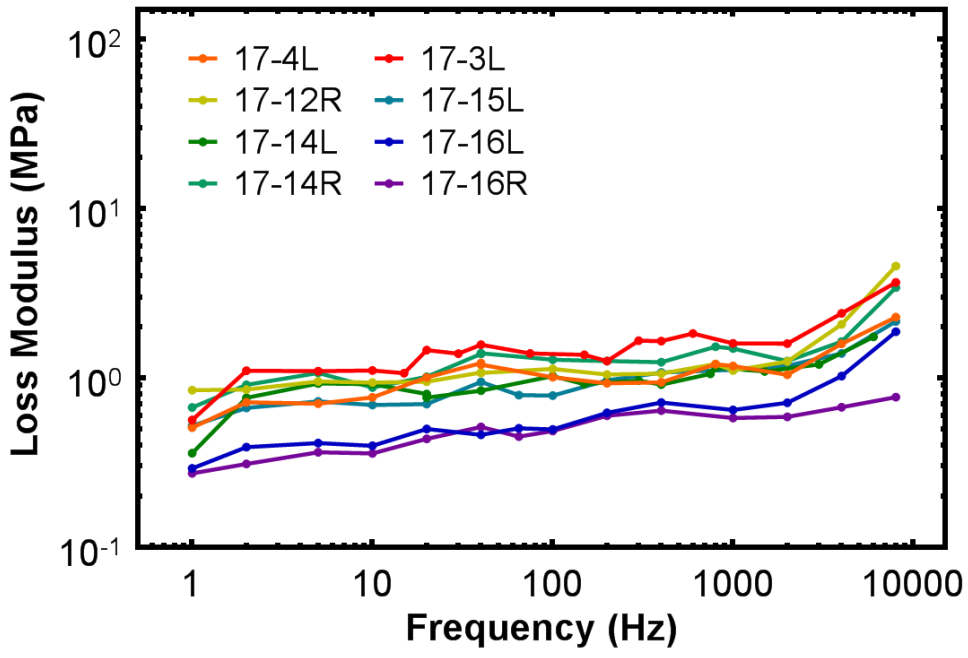

Figure 28. Direct dynamic measurement of the loss modulus in high frequency using FTS for adult baboons.

Table 13. The shift factors and activation energies of adult baboon TM samples.

TM Specimen	α_{25} (25-37)	α_5 (5-37)	$\ln\alpha_{25}$	$\ln\alpha_5$	Ea (kJ/mol)
17-3L	15.0	200.0	2.71	5.30	118.63
17-4L	20.0	200.0	3.00	5.30	118.63
17-14L	20.0	150.0	3.00	5.01	112.19
17-15L	10.0	200.0	2.30	5.30	118.63
17-16L	10.0	200.0	2.30	5.30	118.63
17-16R	10.0	200.0	2.30	5.30	118.63
17-12R	20.0	200.0	3.00	5.30	118.63
17-14R	20.0	200.0	3.00	5.30	118.63
Mean ± SD	15.6 ± 5.0	193.8 ± 17.7	5.70 ± 0.34	5.26 ± 0.10	117.83 ± 2.78

3.3 Failure Experimental Data

After all tests were complete the samples were stretched at a constant rate of 0.1 mm/s until failure. Table 14 through Table 17 lists the ultimate stress or failure stress and stretch ratio for each group of baboons. The mean failure stress for G1 was 2.57 ± 0.66 MPa and the mean failure stretch ratio was 1.21 ± 0.06. The mean failure stress for G2 was 2.56 ± 0.46 MPa and the mean failure stretch ratio was 1.26 ± 0.05. The mean failure stress for G3 was 2.47 ± 0.82 MPa and the mean failure stretch ratio was 1.21 ± 0.05. The mean failure stress for G4 was 2.40 ± 1.06 MPa and the mean failure stretch ratio was 1.21 ± 0.05.

Table 14. Stretch ratio and stress at ultimate stress or failure stress for G1.

TM Specimen	Failure Stretch Ratio λ	Failure Stress (MPa)
16-9L	1.25	1.75
16-9R	1.24	2.44
17-1LP	1.21	3.45
17-1LA	1.15	2.58
17-1R	1.15	3.43
17-18L	1.30	2.41
17-18R	1.17	1.96
Mean ± SD	1.21 ± 0.06	2.57 ± 0.66

Table 15. Stretch ratio and stress at point of failure for G2.

TM Specimen	Failure Stretch Ratio λ	Failure Stress (MPa)
16-8RA	1.26	2.46
16-3RP	1.37	2.35
16-7L	1.25	1.90
16-2LP	1.28	2.50
15-14L	1.27	2.30
17-9L	1.23	3.19
17-9R	1.26	3.27
17-11L	1.17	2.20
17-11R	1.22	2.88
Mean ± SD	1.26 ± 0.05	2.56 ± 0.46

Table 16. Stretch ratio and stress at point of failure for G3.

TM Specimen	Failure Stretch Ratio λ	Failure Stress (MPa)
17-6R	1.22	2.72
17-10R	1.30	3.52
17-7R	1.20	2.14
17-2L	1.14	0.98
17-2R	1.23	3.14
17-3L	1.19	2.53
17-4L	1.18	2.26
Mean ± SD	1.21 ± 0.05	2.47 ± 0.82

Table 17. Stretch ratio and stress at point of failure for G4.

TM Specimen	Failure Stretch Ratio λ	Failure Stress (MPa)
16-6L	1.27	2.94
17-14L	1.18	2.35
17-14R	1.14	3.52
17-12R	1.22	3.77
17-15L	1.23	1.92
17-16L	1.18	1.07
17-16R	1.28	1.23
Mean ± SD	1.21 ± 0.05	2.40 ± 1.06

Chapter 4: Discussion

4.1 Thickness Changes with Age

The thickness was measured using the OCT following the procedure described in section "Thickness measurement with Optical Coherence Tomography" for four baboon age groups: less than 1, 1 to 3, 3 to 5, and older than 5 years of age. The final thickness reported for each TM was an average of six measurements in the pars tensa. For G1, G2, G3, and G4, the average thickness was 0.025 ± 0.004, 0.027 ± 0.009, 0.023 ± 0.003, and 0.024 ± 0.003 mm. No conclusion can be made at this time about changes in the thickness of the TM with age.

4.2 Discussion on Static Results

4.2.1 Uniaxial Tension

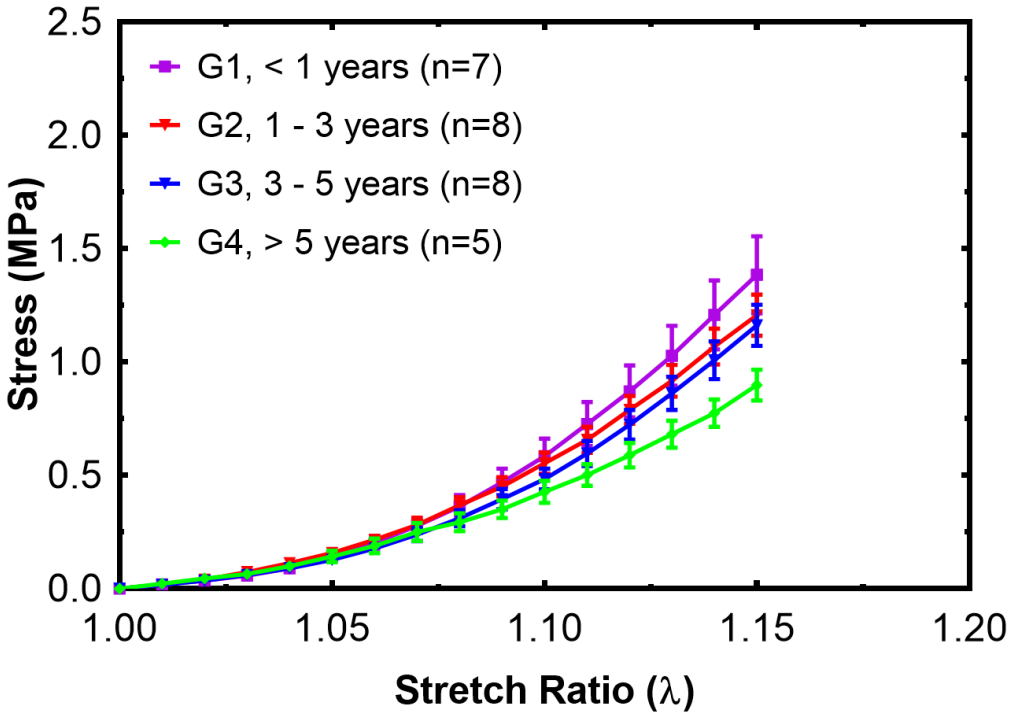

Figure 29. Mean and SE stress for each age group.

The stress-stretch ratio relationship for each age group was plotted as the average and standard error of the mean (SE) in Figure 29. The average stress is relatively equal until 1.05 with the median stress as 0.14 MPa, and at 1.07 they diverge to G1 with the highest average stress, G2 and G3 were second highest, and G4 was the lowest average stress with 1.38 ± 0.17 MPa, 1.21 ± 0.09 MPa, 1.16 ± 0.09 MPa, and 0.90 ± 0.68 MPa.

To test for significance between different groups, a one-way, single-factor ANOVA test was performed with an alpha value of 0.1 which yields a P-value of 0.0837, indicating that within the groups there is significance. The Tukey-Kraemer analysis was performed on 6 pairs from the age groups consisting of G1 vs. G2, G1 vs. G3, G1 vs. G4, G2 vs. G3, G2 vs. G4, G3 vs. G4. The results showed that there was a significant difference between G1 vs. G4, and the results of the ANOVA and Tukey-Kraemer test were summarized in Table 18 in the second column.

Table 18. Summary of quasi-static statistical analysis of 4 age groups.

Type of Test	Tensile Test	Stress Relaxation			Tangent Modulus
Data Point	σ(1.15)	G(25s)	G(70s)	G(150s)	dσ/dλ (1.15)
ANOVA P value	0.0837	0.4280	0.5041	0.6987	0.0523
Tukey G1 vs G2	No	No	No	No	Yes
Tukey G1 vs G3	No	No	No	No	Yes
Tukey G1 vs G4	Yes	No	No	No	Yes
Tukey G2 vs G3	No	No	No	No	No
Tukey G2 vs G4	No	No	No	No	Yes
Tukey G3 vs G4	No	No	No	No	Yes

Note: P value was obtained using one-way ANOVA, and Tukey-Kraemer analysis was used to assess where the significance existed. Tukey-Kraemer does not yield a P value, but a "Yes" will be used to denote significance between groups.

Figure 30 gives the individual curves obtained from fitting the 1st-order Ogden model to the individual stress-strain curves in G1. The maximum predicted stress at the stretch ratio of 1.15 is 2.75 MPa and the lowest predicted stress is 0.82 MPa. The Ogden model parameters are summarized in Table 19 the range of μ_1 values were from 0.30 to 0.79 MPa and the range for α_1 were from 33.94 to 18.84.

The average μ_1 and α_1 values and Eq. 3 can be used to represent the Ogden model for G1 as

$$\sigma = 0.042[(\lambda)^{26.08} - (\lambda)^{-14.54}] \quad (17)$$

Table 19. Ogden hyperelastic 1st order parameters for G1.

TM Specimen	μ_1 (MPa)	α_1
16-9L	0.65	18.84
16-9R	0.30	28.23
17-1LA	0.67	27.59
17-1LP	0.49	30.13
17-1R	0.47	33.94
17-18L	0.60	24.88
17-18R	0.79	25.97
Mean ± SD	0.57 ± 0.16	27.08 ± 4.79

Figure 31 gives the experimentally measured average and standard deviation (SD) from the tension test plotted with the average 1st order hyperelastic Ogden model obtained from curve fitting the individual stress-strain curves. The average Ogden model is well within the SD of the experimental average, which validates an overall good fit. The average SD μ_1 and α_1 were 0.57 ± 0.16 MPa and 27.08 ± 4.79, respectively. At the stress-stretch ratio of 1.03 MPa at 1.13 the Ogden model crosses over the experimental average, and continues rising at a high rate. If the displacement was stretched beyond 15% of the original length it is possible that a higher-order Ogden model may need to be used to predict the stress at higher strain values for G1.

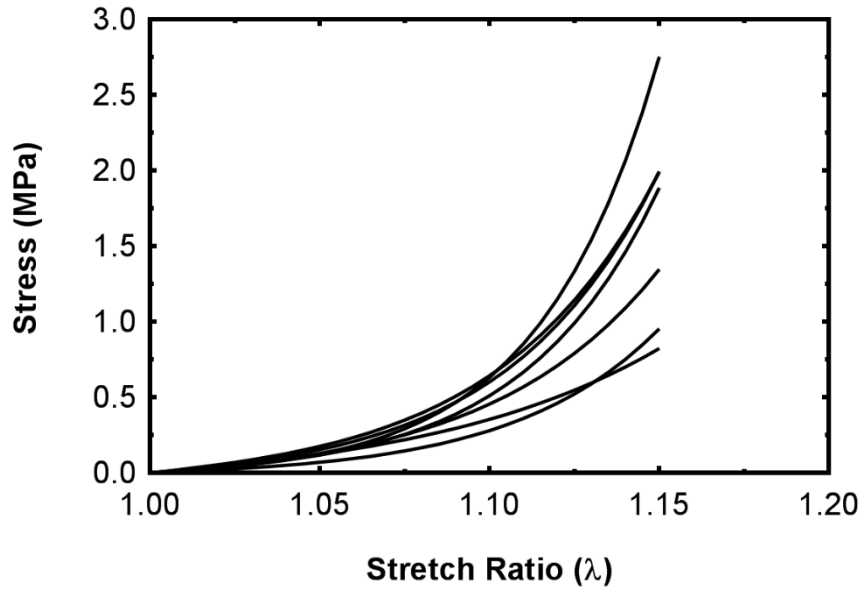

Figure 30. 1st order Ogden model curve fit for G1.

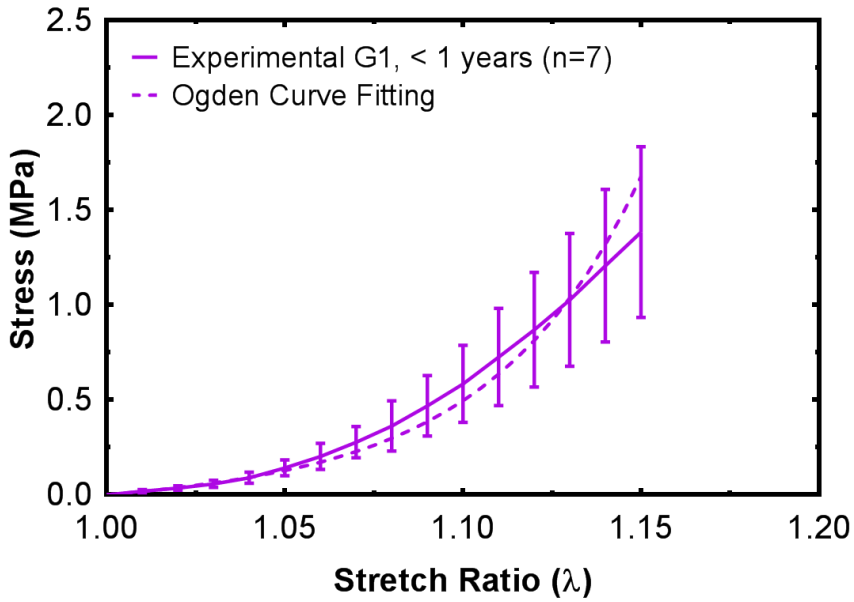

Figure 31. Experimental average and SD (solid) with the average Ogden curve fit (dashed) for G1.

Figure 32 gives the individual curves obtained from fitting the 1st order Ogden model to the individual stress-strain curves in G2. The maximum predicted stress at the

stretch ratio of 1.15 is 1.79 MPa and the lowest predicted stress is 0.86 MPa. The Ogden model parameters are summarized in Table 20 the range of μ_1 values were from 1.08 to 0.35 MPa and the range for α_1 were from 27.28 to 19.48.

The average μ_1 and α_1 values and Eq. 3 can be used to represent the Ogden model for G2 as

$$\sigma = 0.059[(\lambda)^{22.97} - (\lambda)^{-12.99}] \quad (18)$$

Table 20. Ogden hyperelastic 1st order parameters for G2.

TM Specimen	μ_1 (MPa)	α_1
15-14L	0.94	20.48
16-4LP	0.69	25.79
16-7L	0.35	25.66
16-8RA	1.08	19.48
17-9L	0.48	27.28
17-9R	0.42	26.25
17-11L	0.99	21.14
17-11R	0.74	25.67
Mean ± SD	0.71 ± 0.28	23.97 ± 3.06

Figure 33 gives the experimentally measured average and SD for G2 obtained from the tension test plotted with the average 1st-order hyperelastic Ogden model obtained from curve fitting the individual stress-strain curves in G2. As discussed earlier about Figure 31, the average Ogden model is well within the SD of the experimental average of G2, which validates an overall good fit. The average SD μ_1 was 0.71 ± 0.28 MPa and α_1 was 23.97 ± 3.06. At the stress-stretch ratio of 0.92 MPa at 1.13 the Ogden model crosses over the experimental average, and continues rising faster than the experimental average. If the displacement was stretched beyond 15% of the original length it is possible that a higher-order Ogden model may need to be used to predict the stress at higher strain values for G2.

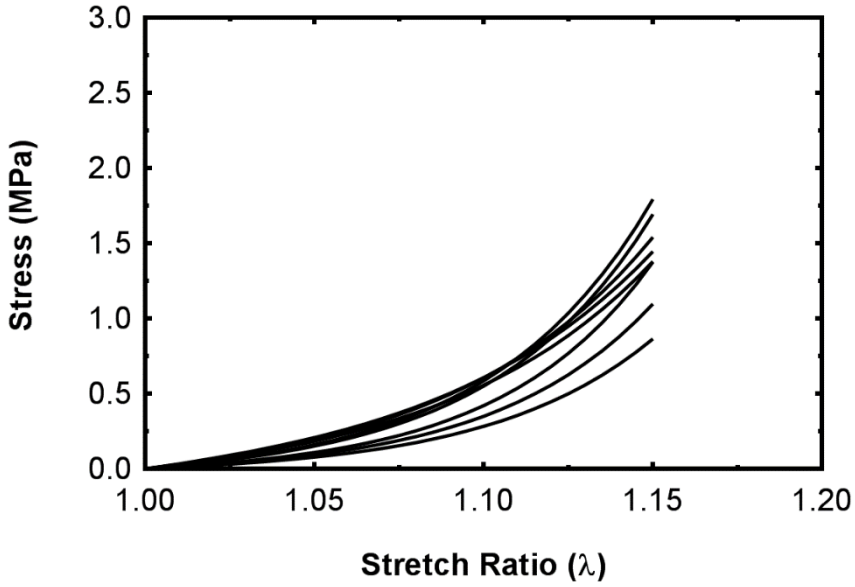

Figure 32. 1st order Ogden model curve fit for G2.

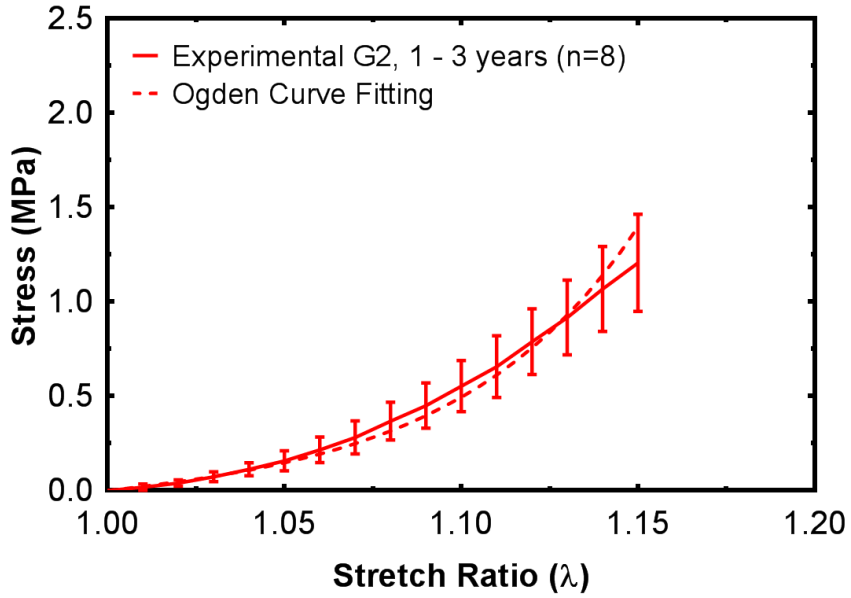

Figure 33. Experimental average and SD (solid) with the average Ogden curve fit (dash) for G2.

Figure 34 gives the individual curves obtained from fitting the 1st order Ogden model to the individual stress-strain curves in G3. The maximum predicted stress at the

stretch ratio of 1.15 is 1.82 MPa and the lowest predicted stress is 0.83 MPa. The Ogden model parameters are summarized in Table 21 the range of μ_1 values were from 0.99 to 0.21 MPa and the range for α_1 were from 34.68 to 19.55.

The average μ_1 and α_1 values and Eq. 3 can be used to represent the Ogden model for G3 as

$$\sigma = 0.045[(\lambda)^{24.83} - (\lambda)^{-13.91}] \quad (19)$$

Table 21. Ogden hyperelastic 1st order parameters for G3.

TM Specimen	μ_1 (MPa)	α_1
17-2L	0.45	22.84
17-2R	0.49	26.82
17-3L	0.99	21.79
17-3R	0.54	26.89
17-4L	0.21	34.68
17-6R	0.93	19.55
17-7R	0.36	27.03
17-10R	0.65	27.03
Mean ± SD	0.58 ± 0.27	25.83 ± 4.60

Figure 35 gives the experimentally measured average and SD for G3 obtained from the tension test plotted with the average 1st order hyperelastic Ogden model obtained from curve fitting the individual stress-strain curves in G3. As seen previously, the average Ogden model is well within the SD of the experimental average, which validates an overall good fit for G3. The average SD μ_1 and α_1 was 0.58 ± 0.27 MPa and 25.83 ± 4.60, respectively. At the stress-stretch ratio of 0.86 MPa at 1.13 the Ogden model crosses over the experimental average, and continues rising faster than the experimental average. If the displacement was stretched beyond 15% of the original length it is possible that a higher order Ogden model may need to be used to predict the stress at higher strain values for G3.

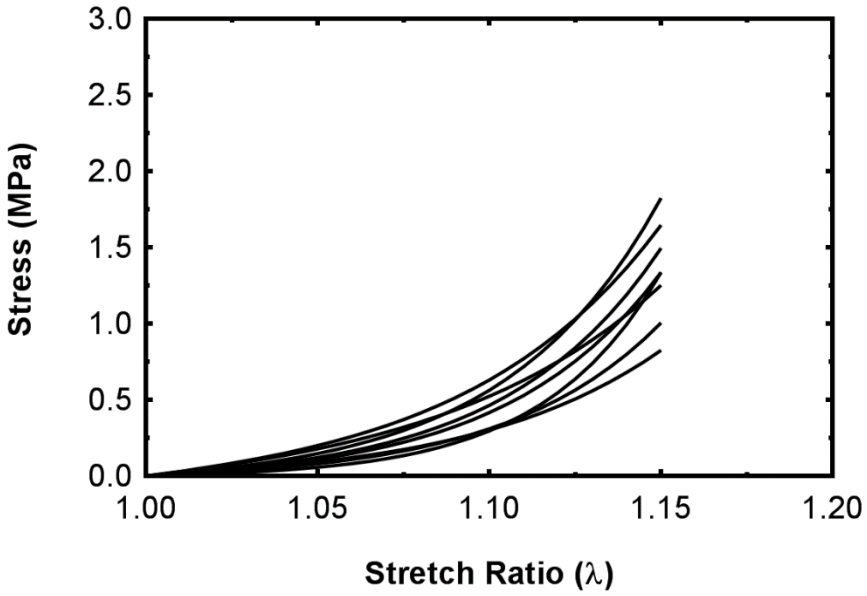

Figure 34. 1st order Ogden model curve fit for G3.

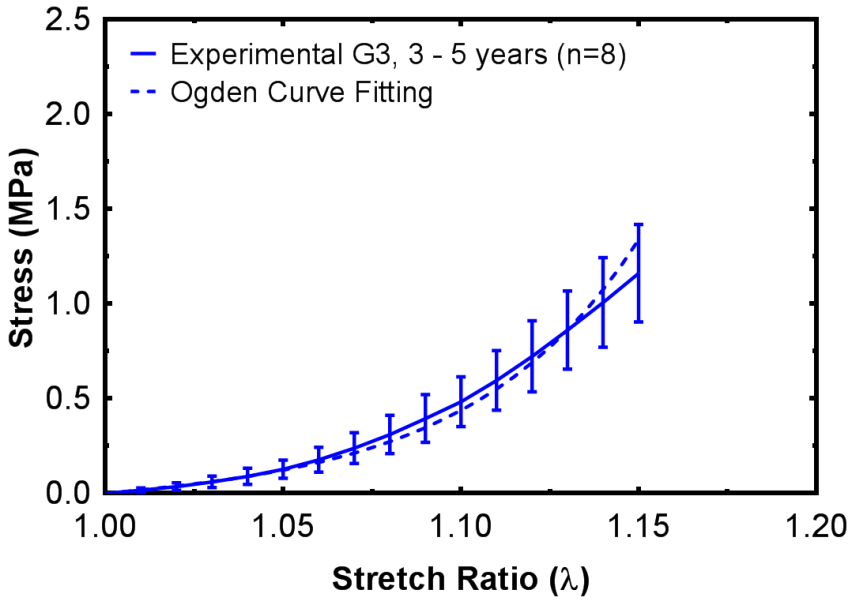

Figure 35. Experimental average and SD (solid) with the average Ogden curve fit (dash) for G3.

Figure 36 gives the individual curves obtained from fitting the 1st-order Ogden model to the individual stress-strain curves in G4. The maximum predicted stress at the stretch ratio of 1.15 is 1.13 MPa and the lowest predicted stress is 0.74 MPa. The Ogden

model parameters are summarized in Table 22 the range of μ_1 values were from 1.17 to 0.29 MPa and the range for α_1 were from 27.05 to 15.39.

The average μ_1 and α_1 values and Eq. 3 can be used to represent the Ogden model for G4 as

$$\sigma = 0.061[(\lambda)^{20.70} - (\lambda)^{-11.85}] \quad (20)$$

Table 22. Ogden hyperelastic 1st order parameters for G4.

TM Specimen	μ_1 (MPa)	α_1
17-14L	0.40	27.05
17-15L	0.63	22.43
17-16L	0.29	26.10
17-16R	0.84	17.54
17-12L	1.17	15.39
Mean ± SD	0.67 ± 0.35	21.70 ± 5.14

Figure 37 gives the experimentally measured average and SD for G4 obtained from the tension test plotted with the average 1st order hyperelastic Ogden model obtained from curve fitting the individual stress-strain curves in G4. As seen previously, the average Ogden model is well within the SD of the experimental average, which validates an overall good fit for G4. The average SD μ_1 was 0.67 ± 0.35 MPa and α_1 was 21.70 ± 5.14. At the stress-stretch ratio of 0.68 MPa at 1.13 the Ogden model crosses over the experimental average, and continues rising faster than the experimental average. If the displacement was stretched beyond 15% of the original length it is possible that a higher-order Ogden model may need to be used to predict the stress at higher strain values for G4.

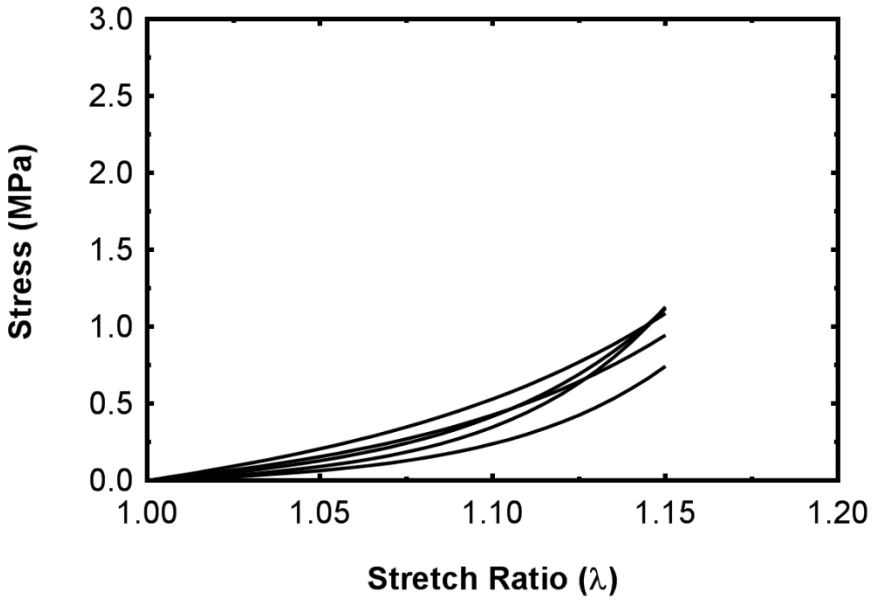

Figure 36. 1st order Ogden model curve fit for G4.

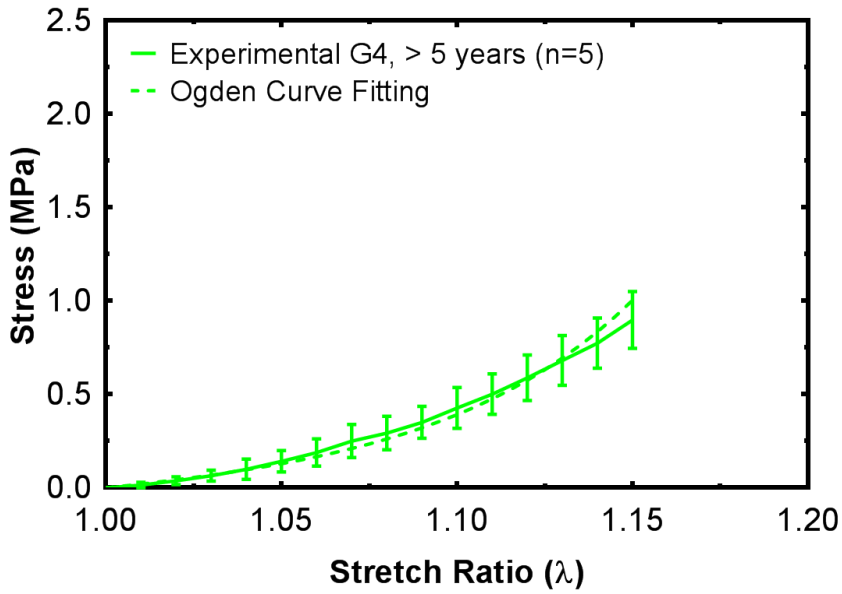

Figure 37. Experimental average and SD (solid) with the average Ogden curve fit (dash) for G4.

Using Eq. 4 and the individual 1st-order Ogden model parameters listed in Table 19 through Table 22, the tangent modulus was obtained for each TM specimen. The tangent modulus can be represented by Eq. 21 through 22

$$\frac{d\sigma}{d\lambda} = 0.042[26.08\lambda^{25.08} - 14.54\lambda^{-15.54}] \quad (21)$$

$$\frac{d\sigma}{d\lambda} = 0.059[22.97\lambda^{21.97} - 12.99\lambda^{-13.99}] \quad (22)$$

$$\frac{d\sigma}{d\lambda} = 0.045[24.83\lambda^{23.83} - 13.91\lambda^{-14.91}] \quad (23)$$

$$\frac{d\sigma}{d\lambda} = 0.061[20.70\lambda^{19.70} - 11.85\lambda^{-12.85}] \quad (24)$$

The average and SE tangent modulus for each baboon age group was plotted in Figure 38. The tangent modulus for all groups were relatively the same at low stretch ratio values for example at 1.05 the median for groups was 3.9 MPa, after 1.05 they diverge to G1 with the highest, G2 and G3 were equal at 2nd highest, and G4 was the lowest average tangent modulus with 40.10 ± 8.15, 28.24 ± 2.46, 29.32 ± 3.18, and 18.49 ± 2.19 MPa, respectively.

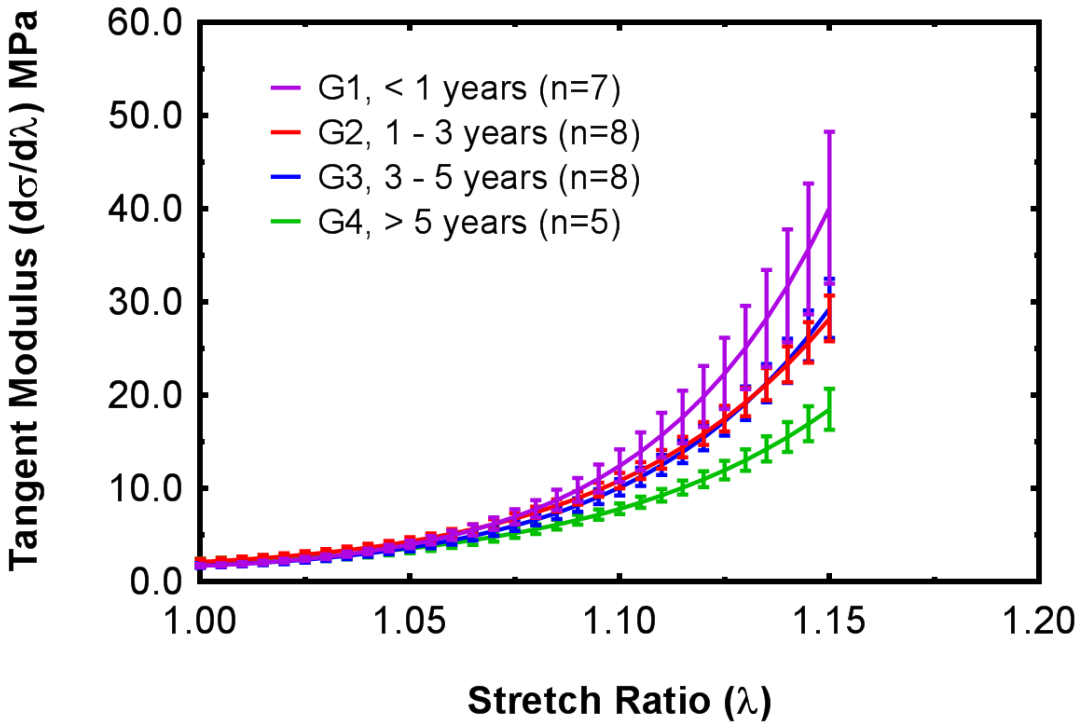

Figure 38. Average and SE tangent modulus for each age baboon group.

To test for significance between the different groups a one-way, single factor ANOVA test was performed with an alpha value of 0.1 which yielded a P value of 0.0523 indicating that within the groups there is significance. The Tukey-Kraemer analysis was performed on 6 pairs from the age groups consisting of G1 vs. G2, G1 vs. G3, G1 vs. G4, G2 vs. G3, G2 vs. G4, G3 vs. G4. The results showed that there was a significant difference between all pairs except G2 vs. G3, which was evident from Figure 38, and the results of the ANOVA and Tukey-Kraemer test were summarized in Table 18 in the 6th column.

To gain a better insight into how stress-stretch ratio relationship of the baboon TM changes with age a separate study done by the Biomedical Engineering Laboratory at the University of Oklahoma performed an experiment using micro-fringe projection.

Images of the fringes were projected onto an intact TM still in the temporal bone, and were acquired by a digital camera connected to a surgical microscope and analyzed using a phase-shift method to reconstruct the surface topography. The relationship between the applied pressure and the resulting volume displacement was determined and analyzed using a finite element model implementing a hyperelastic 2nd-order Ogden model. Through an inverse method, the best-fit model parameters for the TM were determined to allow the simulation results to agree with the experimental data. The nonlinear stress-stretch relationship for the TM of the baboon were determined for 5 age groups: less than 1, 1 to 2, 2 to 3, 3 to 5 and older than 5 years of age [49]. The results can be seen in Figure 39 in comparison to the stress-stretch relationship of the current study. The tangent modulus was obtained for the 2nd order Ogden model and is shown in Figure 40 with the tangent modulus of this study. Although there are differences between this study and the micro-fringe study the important similarity between the studies is that the stress-stretch relation and tangent modulus both show the mechanical properties of the TM decreases with age.

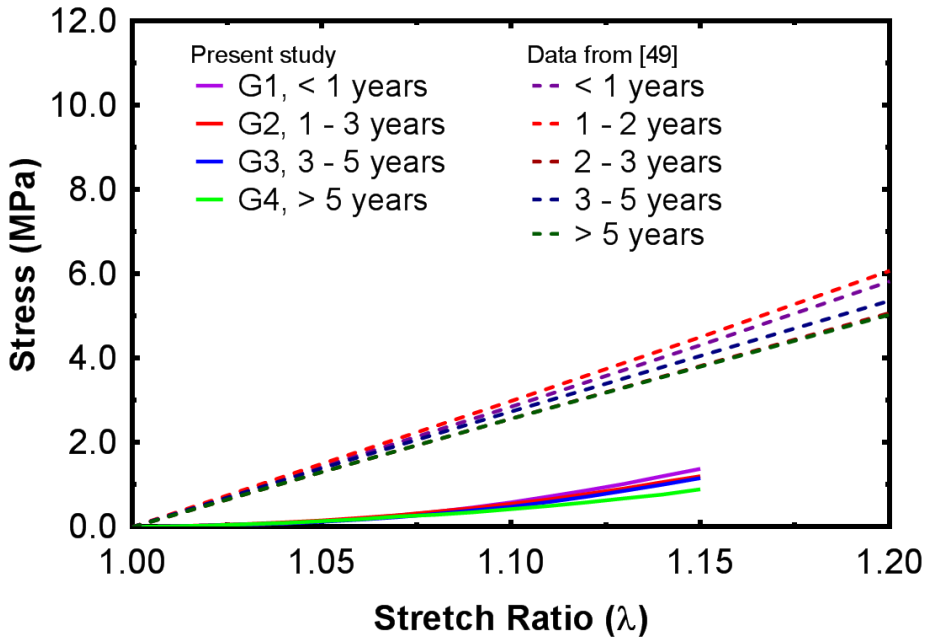

Figure 39. Static micro-fringe and uniaxial tensile stress-stretch ratio relationship of various baboon age groups.

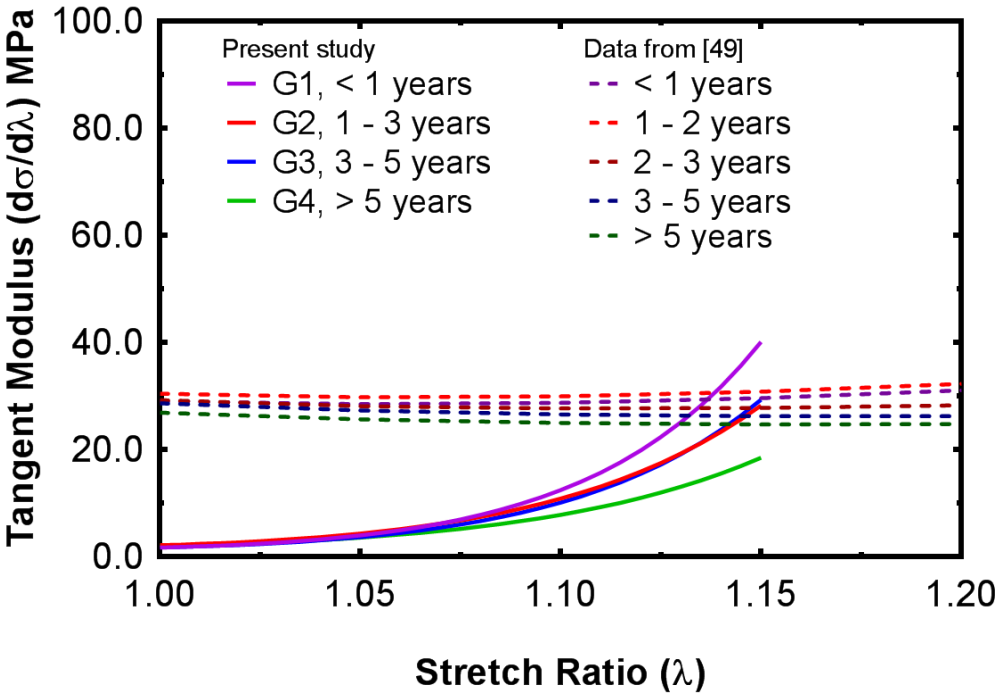

Figure 40. Static micro-fringe and uniaxial tensile tangent modulus-stretch ratio relationship of various baboon age groups.

To elucidate the relationship between the adult baboon and the adult human the stress-stretch ratio relationship for both groups were plotted together within Figure 41. The human data was obtained from a previous study, and consisted of 11 human cadaver subjects that the age ranged from 51 to 92 years old of which 5 were male and 6 were female [7]. In this study, there were 5 baboon subjects that consisted of all female, and the age range was 6 to 15 years, which is approximately 18 to 45 years old in human years. In Figure 41, the average adult baboon is slightly higher than the published human data. However, if additional baboons are tested that are sufficiently older than the current study it may be possible that the stress-stretch ratio relationship will continue to follow the trend observed in Figure 29 and will align with published human data [7].

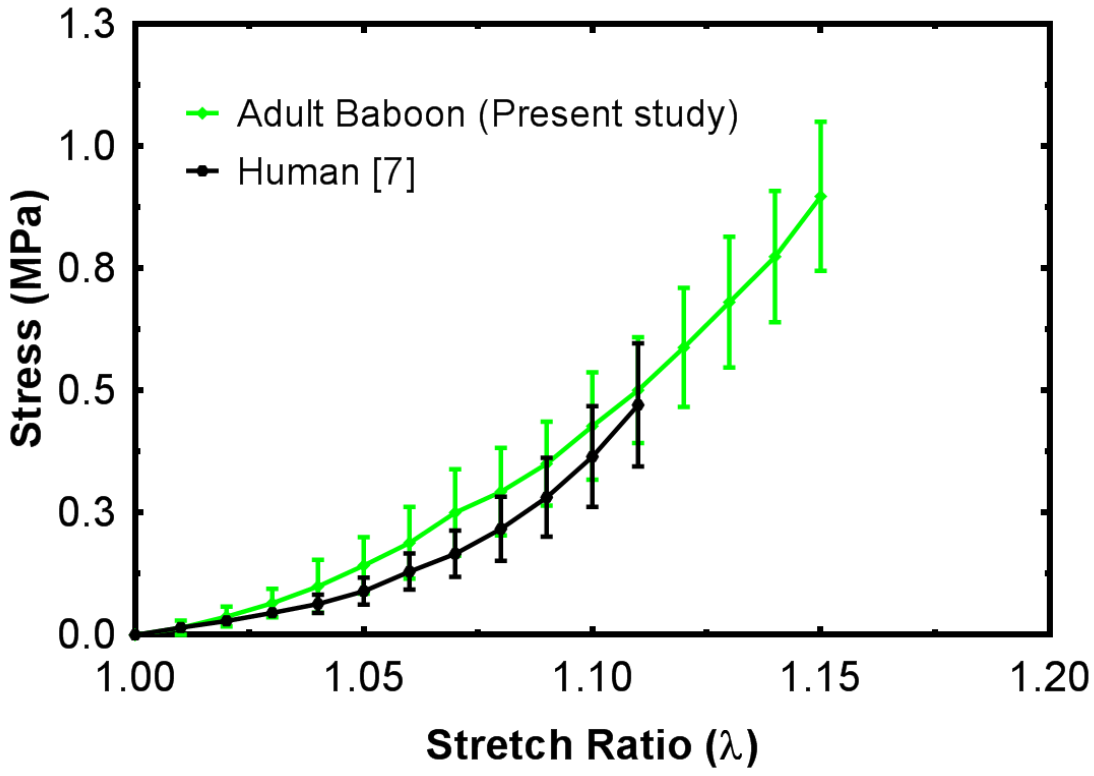

Figure 41. Adult baboon group mean SD in comparison to adult human mean SD.

4.2.2 Relaxation

The average and SE stress relaxation for each group was plotted as in Figure 42. As mentioned before the y-axis is the stress relaxation function G(t) and is defined as the ratio of the stress $\sigma(t)$ at time t and the initial stress σ_0. The strain rate was set to 1.8 mm/s, which was approximately 100 times the strain rate used in the uniaxial tension test.

The stress for all groups decreases with time but reaches relatively stable state after 100 seconds. The rate at which the stress relaxes is relatively fast at the beginning. Within 1 sec, 8% of the median stress is relaxed; at 5 sec, 14% of the median stress is relaxed; at 70 sec, 20% of the median stress is relaxed; after 100 sec the stress is stable at 22% of the median stress is relaxed. The mean relaxed stress after total relaxation was 0.78, 0.78, 0.76, and 0.76 MPa for G1, G2, G3, and G4, respectively. Based on this result of the change of the stress with the time under the constant stretch indicates that the baboon TM at any age range is a viscoelastic material.

To test for significance between the different groups one-way, single factor ANOVA tests were performed at three different time points 25, 50, and 75 sec each with an alpha value of 0.1 which yielded a P value of 0.4280, 0.5041, and 0.6987, respectively, indicating that within the groups there are no significant differences. To be certain, the Tukey-Kraemer analysis was performed on 6 pairs from the age groups consisting of G1 vs. G2, G1 vs. G3, G1 vs. G4, G2 vs. G3, G2 vs. G4, G3 vs. G4. The results showed that none of the pairs were significantly different from each other, and

the results of the ANOVA and Tukey-Kraemer test were summarized in Table 18 in the third, fourth, and fifth column.

Figure 43 shows the relationship between the stress relaxation behavior of the TM in the adult baboon and published adult human [7]. As mentioned previously, the human data consisted of 9 human cadaver subjects that the age ranged from 51 to 92 years old of which 5 were male and 6 were female (the study did not mention which samples were absent from the uniaxial tension test) [7]. In this study, there were 5 baboon subjects that consisted of all female, and the age range was 6 to 15 years, which is approximately 18 to 45 years old in human years. Cheng et al. reported the stress relaxation behavior was, "within 1 sec, 10% of the stress is relaxed; at 5 sec, 20% of the stress is relaxed; after 50 sec, the stress relaxation gradually tends stable and finally, on average, 35% of the stress is totally relaxed" [7]. The adult baboon relaxed at relatively the same rate, but less of the stress was relaxed at each time point.

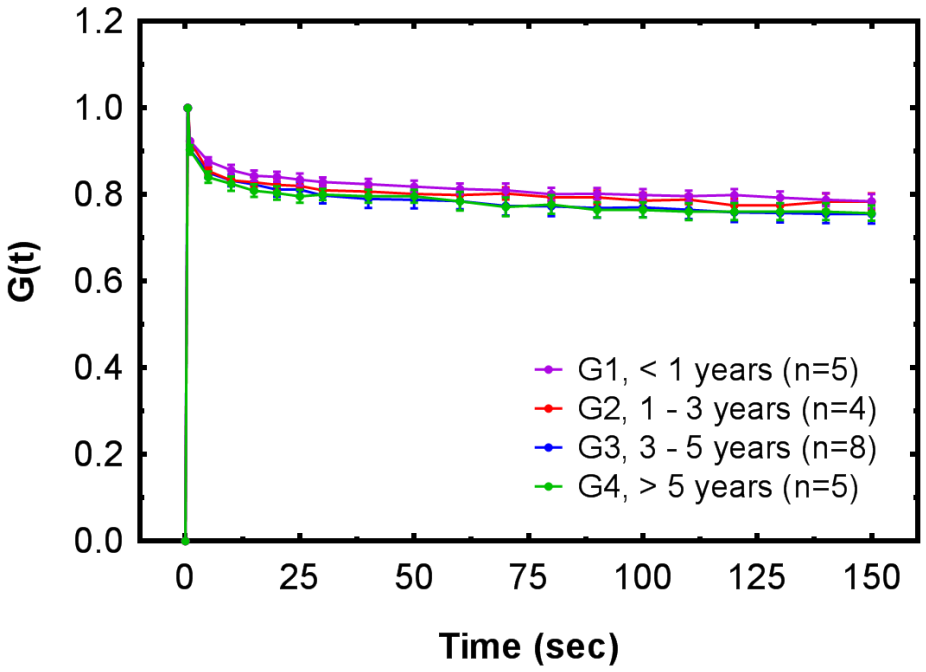

Figure 42. Normalized mean stress relaxation for each group.

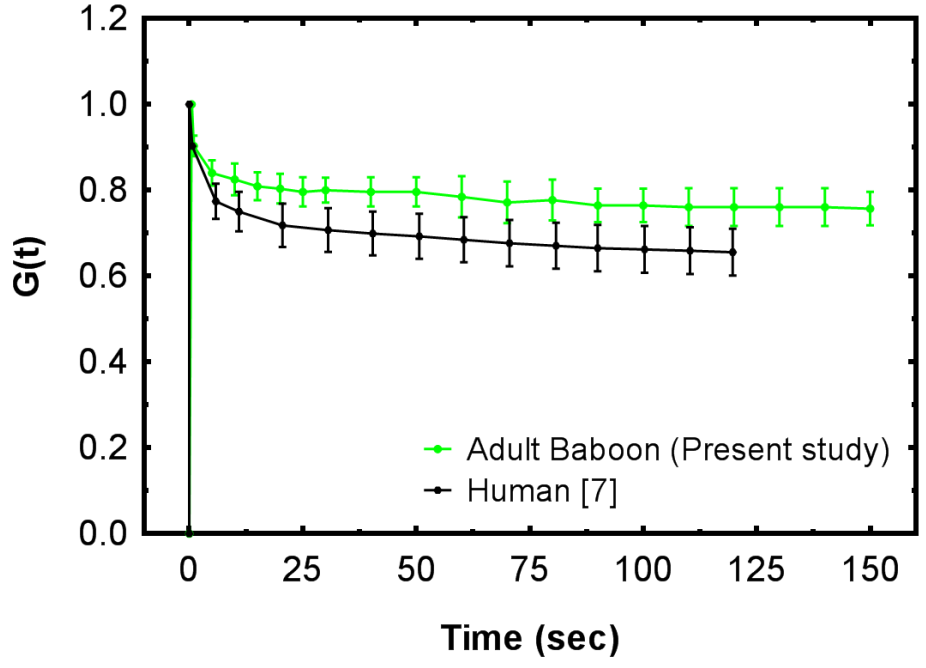

Figure 43. Normalized mean SD for adult baboon in comparison to adult human.

4.3 Discussion on Dynamic Test Results

4.3.1 Low-Frequency

The average SE complex modulus in the low-frequency range from 1 to 80 Hz was plotted for each baboon age group in Figure 44. For each age group the storage modulus is represented as a solid line and the loss modulus is represented as a dashed line. At 1 Hz to 20 Hz the storage modulus are relatively stable with the median storage modulus of the pediatric group of baboons at 11.62 MPa, which is higher than the storage modulus of the adult baboon group at 7.88 ± 0.79 MPa. From 20 to 80 Hz the storage modulus of all 4 groups increase to a median storage modulus of 19.76 MPa. The median loss modulus of the pediatric group of baboons at 1 Hz as 1.48 MPa, which is higher than the loss modulus of the adult baboon group at 1 Hz as 0.60 ± 0.10 MPa. From 20 to 80 Hz the loss modulus of all 4 groups increase to a median loss modulus of 5.91 MPa.

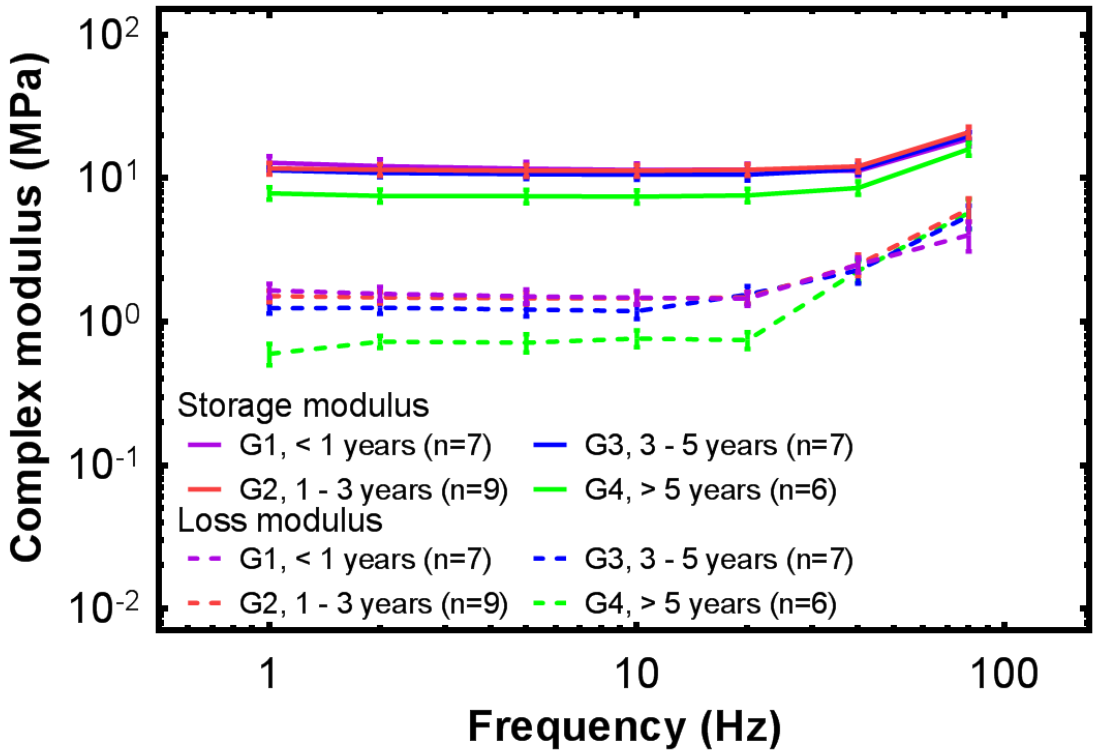

Figure 44. Complex modulus mean for each age group.

To test for significance between the different groups one-way, single factor ANOVA tests were performed on both the storage and loss modulus at three different frequencies 1, 20, and 80 Hz each with an alpha value of 0.1. ANOVA tests on the storage modulus yielded a P value of 0.0313 for 1 Hz, 0.0610 for 20 Hz, and 0.2937 for 80 Hz. ANOVA tests on the loss modulus for 1, 20, and 80 Hz yielded a P value of 0.0002, 0.0104, and 0.4108, respectively. This indicated that the storage and loss modulus at 1 and 20 Hz were was at least some significance. The Tukey-Kraemer analysis was performed for the frequencies 1, 20, and 80 Hz on 6 pairs from the age groups consisting of G1 vs. G2, G1 vs. G3, G1 vs. G4, G2 vs. G3, G2 vs. G4, G3 vs. G4. The results for the storage modulus are that the significantly different pairs were G1 vs. G4 and G2 vs. G4 at 1 and 20 Hz, and there was no significant difference at 80 Hz.

However, the loss modulus showed that there was a significant difference between G1 vs. G4, G2 vs. G4, and G3 vs. G4 at 1 and 20 Hz, but there was no significant difference at 80 Hz among any of the pairs. The results of the ANOVA and Tukey-Kraemer test were summarized in Table 23.

Table 23. Summary of low-frequency statistical analysis of the 4 age groups.

Type of Test	Storage Modulus at Low-Frequency			Loss Modulus at Low-Frequency		
Data Point	1 Hz	20 Hz	80 Hz	1 Hz	20 Hz	80 Hz
ANOVA P value	0.0313	0.0610	0.2937	0.0002	0.0104	0.4108
Tukey G1 vs G2	No	No	No	No	No	No
Tukey G1 vs G3	No	No	No	No	No	No
Tukey G1 vs G4	Yes	Yes	No	Yes	Yes	No
Tukey G2 vs G3	No	No	No	No	No	No
Tukey G2 vs G4	Yes	Yes	No	Yes	Yes	No
Tukey G3 vs G4	No	No	No	Yes	Yes	No

Note: P value was obtained using one-way ANOVA, and Tukey-Kraemer analysis was used to assess where significance existed. Tukey-Kraemer does not yield a P value, but a "Yes" will be used to denote significance between groups.

4.3.2 Frequency-Temperature Superposition

Two samples from G3 (17-3L and 17-4L both are 4.5 years old) were used in the FTS experiment to observe how much crossover might occur between age groups. In Figure 27 showed that the storage modulus for the two samples were very similar to the group average. In Figure 28 the loss modulus for 17-4L was very close to the group average, and in the same figure 17-3L was higher than most samples but still within the groups SD. However, the two oldest samples in the group were 17-16L and 17-16R both of which were 15 years old. In both figures they can be seen as having the lowest storage and loss modulus of the group. It is possible that as the baboon ages past 10

years there is a severe decrease in the complex modulus of the TM, and a future study will need to limit the FTS method to only samples that are at least 15 years old.

To elucidate the relationship between the adult baboon and the adult human the complex modulus for both groups were plotted together within Figure 45. The human data was obtained from a previous study and consisted of 11 human cadaver subjects that the age ranged from 64 to 74 years old of which 5 were female and 1 was male [13]. In this study there were 8 baboon subjects that consisted of 7 female and 1 male, and the age range was 4.5 to 15 years, which is approximately 14 to 45 years old in human years.

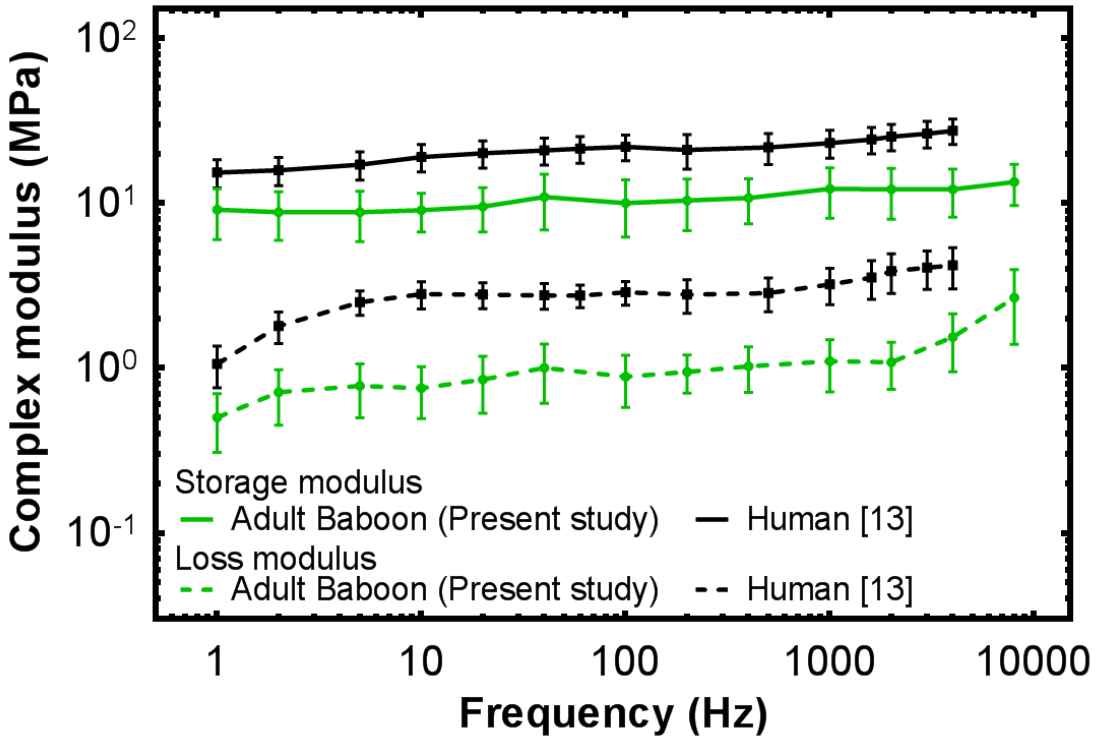

Figure 45. Complex modulus average SD in high frequency obtained with FTS of adult baboon compared to adult human.

The average storage modulus at 1 Hz for the baboon was 9.12 ± 3.12 MPa and the human was 15.32 ± 2.99 MPa; at 100 Hz, the baboon was 10.02 ± 3.80 MPa and the human was 21.94 ± 3.89 MPa; at 1000 Hz, the baboon was 12.23 ± 4.13 MPa and the human was 23.16 ± 4.45 MPa; finally at the upper range of the human complex modulus of 4000 Hz the baboon storage modulus was 12.15 ± 3.93 MPa and the human was 27.49 ± 4.84 MPa. The average loss modulus at 1 Hz for the baboon was 0.50 ± 0.20 MPa and the human was 1.06 ± 0.30; at 100 Hz, the baboon was 0.89 ± 0.31 MPa and the human was 2.88 ± 0.47 MPa; at 1000 Hz, the baboon was 1.10 ± 0.38 MPa and the human was 3.22 ± 0.80 MPa; finally at 4000 Hz, the baboon was 1.54 ± 0.59 MPa and the human was 4.19 ± 1.17 MPa.

4.4 Scanning Electron Microscopy of Adult Baboon TM

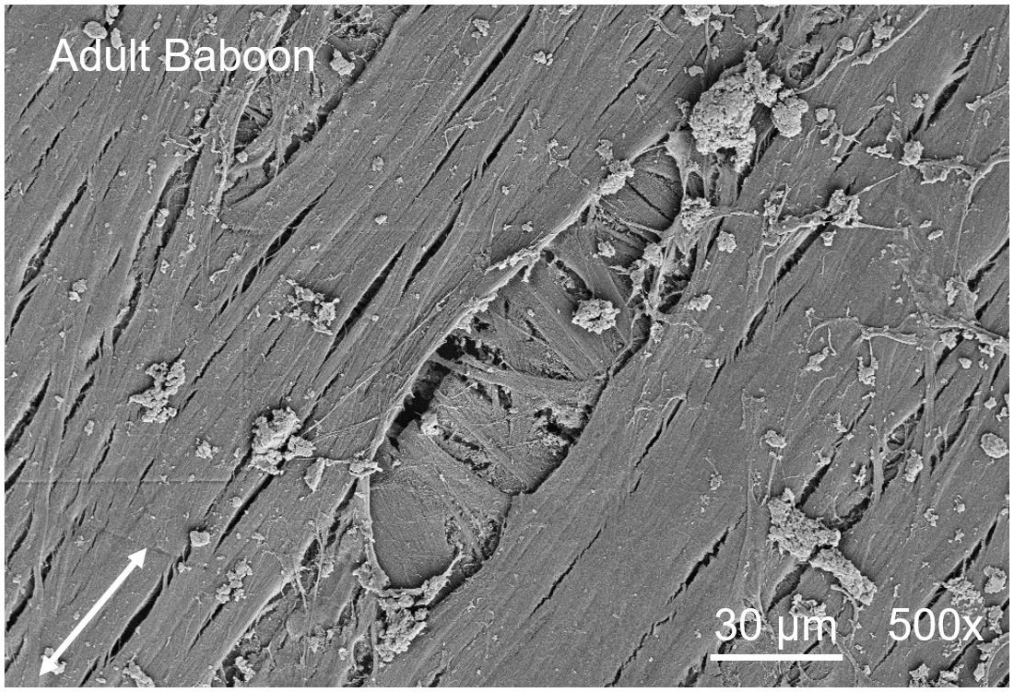

Figure 46. SEM image of baboon TM. Radial direction is indicated by double sided arrow.

Figure 46 shows the image obtained from SEM. The figure is currently at 500 times zoom, and the orientation of the radial fibers is indicated by the double-sided arrow. The image was focuses on an area of the TM where the radial fibers separated slightly, which was due to the process that prepares the TM for SEM imaging. In this separation, there can be a different set of fibers that are running in the circumferential direction.

4.5 Study Limitations

A major concern about the study is with respect to the freshness of the samples. As such great care was taken to insure the freshness and validity of the sample until testing. There have been studies that focused on the effect of freezing and thawing samples had on tissue, and the results showed that the mechanical properties of collagen does not change at the micro- or macro-scale [50]. Additionally, a separate pilot study was done to observe the effect of freezing and thawing had on samples and found that were was no significant change in the mechanical properties of the tissues tested.

In this study, the specimens were taken either from the posterior or anterior site of the TM and the loading for all experiments was along the superior-inferior or longitudinal direction of the specimens. The TM was considered as an isotropic and homogenous material for macro-mechanics study. However, it was observed from Figure 46 that the TM is at least a two-layer structure of radial and circumferential fibers. Furthermore, because the human TM is a multi-layer structure with collage fibers along radial and circumferential directions it can be deduced that between this evidence

and Figure 46 that the baboon TM is composed of a similar structure [51]. The ultrastructure of the baboon TM should be considered in mechanical measurements.

Finally, there is no precedent for the study of baboon middle ear mechanics. Therefore any result obtained can only be compared to the results obtained from other species such as the chinchilla and human. However, this is still a great first step, and the change in the mechanical properties of the TM with age can be further studied using a large sample size or by using different experimental methods.

Chapter 5: Conclusion

5.1 Summary of Findings

In order to determine the effect age on the mechanical properties of the baboon TM, four age groups were establish: less than 1, 1 to 3, 3 to 5, and older than 5 years of age. Several experiments were conducted for each age group, starting with quasi-static testing uniaxial tension, and stress relaxation tests, and followed by direct measurement of the complex modulus in the low frequency range of 1 to 80 Hz. The adult baboon group was additionally tested in the auditory frequency range by using the FTS principle which measures the complex modulus at the frequencies 1, 2, 5, 10, 20, and 40 Hz at three different temperatures 5°C, 25°C, and 37°C. Then using a shift factor the complex modulus associated with the lower temperatures are shifted into the higher frequency range with a reference temperature of 37°C. Quasi-static and dynamic testing revealed that as the baboon TM ages the mechanical properties decrease. The stress-stretch ratio relationship obtained from the uniaxial tension test showed that the adult baboon was significantly lower than the pediatric age range. For all age groups, the individual stress-strain curves obtained from the uniaxial tension test were fitted with a 1^{st} order hyperelastic Ogden model, and the paramters were used to obtain the tangent modulus-strain relationship. The youngest group had the highest, the oldest group had the lowest tangent modulus. The baboon groups with an age range of 1 to 3 and 3 to 5 years of age were statistically the same as each other, but between the youngest and oldest baboon samples. Therefore, the conclusion is that the tangent modulus decreases with age. The stress relaxation modulus was statistically the same across all age groups. The direct measurement of the complex modulus in the low frequency range of 1 to 80

Hz showed that as the baboon ages the storage modulus and loss modulus decreased but only after 5 years of age. The age groups that were less than 1, 1 to 3, and 3 to 5 years of age had the same complex modulus, but were significantly higher than the adult baboon group for frequencies 1 through 20 Hz.

5.2 Future Studies

This study focused on the mechanical properties obtained for quasi-static and low frequency testing from young to adult baboon TMs, and also obtained the complex modulus for the adult baboon TM. However, an additional study can be done to measure the complex modulus in the auditory frequency range for each baboon group instead of just the adult group. This allow for a better understanding of how the complex modulus changes with age across the entire frequency range instead of just 1 to 80 Hz. An additional study can be done to further support evidence of how the complex modulus changes with age. For instance, instead of using the DMA coupled with the FTS principle to directly measure the complex modulus in the auditory frequency range the acoustic driving with inverse problem-solving method can be used. The method is conducted by measuring the vibration of the TM strip specimen induced by acoustic loading and measured by laser Doppler vibrometry (LDV) over a frequency range of 200-8000 Hz. Then an inverse-problem solving method with finite element modeling is used to determine the complex modulus of the TM specimen. This method has been used to measure the TM and other soft tissues of the middle ear [12]. Understanding how the mechanical properties of the TM changes with age is a great first step to how the ear changes with age. However, to achieve a better understanding additional soft

tissues of the ear should be studied in different age groups. Soft tissues that need further study are the suspensory ligaments tendons, incudomalleolar joint, incudostapedial joint, and stapedial annular ligament. Once the mechanical properties of these soft tissues are known they can be used as inputs into the adult and infant baboon model developed by Biomedical Engineering Laboratory at the University of Oklahoma [25]. With that additional simulations can be performed on how sound transmission will be affected by age and pathologies at different ages.

References

[1] Fung, Yuan-cheng. *Biomechanics: mechanical properties of living tissues*. Springer Science & Business Media, 2013.

[2] Schilder, Anne GM, Tal Marom, Mahmood F. Bhutta, Margaretha L. Casselbrant, Harvey Coates, Marie Gisselsson-Solén, Amanda J. Hall et al. "Panel 7: Otitis Media: Treatment and Complications." *Otolaryngology–Head and Neck Surgery* 156, no. 4_suppl (2017): S88-S105.

[3] Luers, Jan Christoffer, and Karl- Bernd Hüttenbrink. "Surgical anatomy and pathology of the middle ear." *Journal of anatomy* 228, no. 2 (2015): 338-353.

[4] Mansour, Salah, Jacques Magnan, Hassan Haidar, Karen Nicolas, and Stéphane Louryan. *Comprehensive and clinical anatomy of the middle ear*. Springer Berlin Heidelberg, 2013.

[5] Keefe, D. H., M. P. Feeney, J. Katz, L. Medwetski, R. Burkard, and L. Hood. "Principles of acoustic immittance and acoustic transfer functions." *Handbook of clinical audiology* (2009): 125-156.

[6] Von Békésy, Georg. *Experiments in Hearing.* Oxford, England: Mcgraw Hill, 1960.

[7] Cheng, Tao, Chenkai Dai, and Rong Z. Gan. "Viscoelastic Properties of Human Tympanic Membrane." *Annals of Biomedical Engineering* 35, no. 2 (December 8, 2006): 305–14.

[8] Daphalapurkar, Nitin P., Chenkai Dai, Rong Z. Gan, and Hongbing Lu. "Characterization of the Linearly Viscoelastic Behavior of Human Tympanic Membrane by Nanoindentation." *Journal of the Mechanical Behavior of Biomedical Materials* 2, no. 1 (January 2009): 82–92.

[9] Fay, Jonathan, Sunil Puria, Willem F. Decraemer, and Charles Steele. "Three approaches for estimating the elastic modulus of the tympanic membrane." *Journal of biomechanics* 38, no. 9 (2005): 1807-1815.

[10] Huang, Gang, Nitin P. Daphalapurkar, Rong Z. Gan, and Hongbing Lu. "A Method for Measuring Linearly Viscoelastic Properties of Human Tympanic Membrane Using Nanoindentation." *Journal of Biomechanical Engineering* 130, no. 1 (February 1, 2008): 014501–014501.

[11] Kirikae, Ichiro. *The Structure and Function of the Middle Ear*. Tokyo: University Press, 1960.

[12] Zhang, Xiangming, and Rong Z. Gan. "Dynamic Properties of Human Tympanic Membrane – Experimental Measurement and Modelling Analysis." *International Journal of Experimental and Computational Biomechanics* 1, no. 3 (January 1, 2010): 252–70.

[13] Zhang, Xiangming, and Rong Z. Gan. “Dynamic Properties of Human Tympanic Membrane Based on Frequency-Temperature Superposition.” *Annals of Biomedical Engineering* 41, no. 1 (July 21, 2012): 205–14.

[14] Luo, Huiyang, Chenkai Dai, Rong Z. Gan, and Hongbing Lu. “Measurement of Young’s Modulus of Human Tympanic Membrane at High Strain Rates.” *Journal of Biomechanical Engineering* 131, no. 6 (April 29, 2009): 064501–064501.

[15] Dormehl, I. C., N. Hugo, and G. Beverley. “The Baboon: An Ideal Model in Biomedical Research.” *Anesthesia & Pain Control in Dentistry* 1, no. 2 (1992): 109–15.

[16] Luck, Jason F., Roger W. Nightingale, Andre M. Loyd, Michael T. Prange, Alan T. Dibb, Yin Song, Lucy Fronheiser, and Barry S. Myers. "Tensile mechanical properties of the perinatal and pediatric PMHS osteoligamentous cervical spine." *Stapp car crash journal* 52 (2008): 107.

[17] Grow, Douglas A., John R. McCarrey, and Christopher S. Navara. “Advantages of Nonhuman Primates as Preclinical Models for Evaluating Stem Cell-Based Therapies for Parkinson’s Disease.” *Stem Cell Research* 17, no. 2 (September 2016): 352–66.

[18] Nyachieo, Atunga, Daniel C. Chai, Jan Deprest, Jason M. Mwenda, and Thomas M. D’Hooghe. “The Baboon as a Research Model for the Study of Endometrial Biology, Uterine Receptivity and Embryo Implantation.” *Gynecologic and Obstetric Investigation* 64, no. 3 (2007): 149–55.

[19] Fazleabas, A. T., J. J. Kim, S. Srinivasan, K. M. Donnelly, A. Brudney, and R. C. Jaffe. “Implantation in the Baboon: Endometrial Responses.” *Seminars in Reproductive Endocrinology* 17, no. 3 (1999): 257–65.

[20] Wright, C. G., A. R. Halama, and W. L. Meyerhoff. “Ototoxicity of an Ototopical Preparation in a Primate.” *The American Journal of Otology* 8, no. 1 (January 1987): 56–60.

[21] Wright, C. G., W. L. Meyerhoff, and A. R. Halama. “Ototoxicity of Neomycin and Polymyxin B Following Middle Ear Application in the Chinchilla and Baboon.” *The American Journal of Otology* 8, no. 6 (November 1987): 495–99.

[22] Martin, G. K., B. L. Lonsbury-Martin, R. Probst, and A. C. Coats. “Spontaneous Otoacoustic Emissions in the Nonhuman Primate: A Survey.” *Hearing Research* 20, no. 1 (1985): 91–95.

[23] Geyer, G., and J. Helms. “[Ionomer Cement Prostheses in Reconstructive Middle Ear Surgery].” *HNO* 45, no. 6 (June 1997): 442–47.

[24] Moore, J. K., K. K. Osen, J. Storm-Mathisen, and O. P. Ottersen. "Gamma-Aminobutyric Acid and Glycine in the Baboon Cochlear Nuclei: An Immunocytochemical Colocalization Study with Reference to Interspecies Differences in Inhibitory Systems." *The Journal of Comparative Neurology* 369, no. 4 (June 10, 1996): 497–519.

[25] Hitt, Brooke M. *Modeling and Measurement of Sound Transmission in the Baboon Ear*, 2017. https://hdl.handle.net/11244/50845

[26] Reddy, Junuthula Narasimha. *An introduction to the finite element method*. Vol. 2, no. 2.2. New York: McGraw-Hill, 1993.

[27] R. Gan, B. Reeves and X. Wang, "Modeling of Sound Transmission from Ear Canal to Cochlea." *Annals of Biomedical Engineering*, vol. 35, no. 12, (2007): 2180-2194.

[28] R. Gan, T. Cheng, C. Dai and F. Yang, "Finite Element Modeling of Sound Transmission with Perforations of Tympanic Membrane." *The Journal of the Acoustic Society of America*, vol. 126, no. 1, (2009): 243-253.

[29] R. Gan, B. Feng and Q. Sun, "3-Dimensional Finite Element Modeling of Human Ear for Sound Transmission." *Annals of Biomedical Engineering*, vol. 32, no. 6, (2004): 847-856.

[30] X. Zhang and R. Gan, "Finite Element Modeling of Energy Absorbance in Normal and Disordered Human Ears." *Hearing Research*, vol. 301, (2013): 146-155.

[31] Gan, Rong Z., Chenkai Dai, Xuelin Wang, Don Nakmali, and Mark W. Wood. "A totally implantable hearing system–design and function characterization in 3D computational model and temporal bones." *Hearing research* 263, no. 1 (2010): 138-144.

[32] T. Koike, H. Wada, and T. Kobayashi, "Modeling of the Human Middle Ear Using the Finite-Element Method." *The Journal of the Acoustic Society of America*, vol. 111, no. 3, (March 2002): 1306–1317.

[33] R. Z. Gan, D. Nakmali, X. D. Ji, K. Leckness, and Z. Yokell, "Mechanical Damage of Tympanic Membrane in Relation to Impulse Pressure Waveform – A Study in Chinchillas." *Hearing Research*, vol. 340, (October 2016): 25–34.

[34] G. Viallet, G. Sgard, F. Laville and J. Boutin, "Axisymmetic versus Three-Dimensional Finite Element Models for Predicting the Attenuation of Earplugs in Rigid Walled Ear Canals." *The Journal of the Acoustic Society of America*, vol. 134, no. 6, (2003): 4470-4480.

[35] Jiang, Shangyuan, Thomas W. Seale, and Rong Z. Gan. "Morphological Changes in the Round Window Membrane Associated with Haemophilus Influenzae-

Induced Acute Otitis Media in the Chinchilla.” *International Journal of Pediatric Otorhinolaryngology* 88 (September 2016): 74–81.

[36] Zhou, Yifeng, Kenny KH Chan, Tom Lai, and Shuo Tang. "Characterizing refractive index and thickness of biological tissues using combined multiphoton microscopy and optical coherence tomography." *Biomedical optics express* 4, no. 1 (2013): 38-50.

[37] Chan, Roger W. "Estimation of viscoelastic shear properties of vocal-fold tissues based on time–temperature superposition." *The Journal of the Acoustical Society of America* 110, no. 3 (2001): 1548-1561.

[38] Peters, G. W. M., J. H. Meulman, and A. A. H. J. Sauren. "The applicability of the time/temperature superposition principle to brain tissue." *Biorheology* 34, no. 2 (1997): 127-138.

[39] Sarma, P. A., R. M. Pidaparti, P. N. Moulik, and R. A. Meiss. "Non- linear material models for tracheal smooth muscle tissue." *Bio-medical materials and engineering* 13, no. 3 (2003): 235-245.

[40] Miller, Karol, and Kiyoyuki Chinzei. "Mechanical properties of brain tissue in tension." *Journal of biomechanics* 35, no. 4 (2002): 483-490.

[41] Wu, John Z., Ren G. Dong, W. Paul Smutz, and Aaron W. Schopper. "Nonlinear and viscoelastic characteristics of skin under compression: experiment and analysis." *Bio-medical materials and engineering* 13, no. 4 (2003): 373-385.

[42] Ogden, Raymond William. "Large deformation isotropic elasticity–on the correlation of theory and experiment for incompressible rubberlike solids." In *Proc. R. Soc. Lond. A*, 326, no. 1567 (1972): 565-584.

[43] Ferry, John D. "Mechanical properties of substances of high molecular weight. VI. Dispersion in concentrated polymer solutions and its dependence on temperature and concentration." *Journal of the American Chemical Society* 72, no. 8 (1950): 3746-3752.

[44] Williams, Malcolm L., Robert F. Landel, and John D. Ferry. "The temperature dependence of relaxation mechanisms in amorphous polymers and other glass-forming liquids." *Journal of the American Chemical society* 77, no. 14 (1955): 3701-3707.

[45] Ferry, John D. *Viscoelastic properties of polymers*. John Wiley & Sons, 1980.

[46] Radebaugh, Galen W., and Anthony P. Simonelli. "Temperature—frequency equivalence of the viscoelastic properties of anhydrous lanolin usp." *Journal of pharmaceutical sciences* 72, no. 4 (1983): 422-425.

[47] Nielsen, L. E., and R. F. Landel. Mechanical Properties of Polymers and Composites (2nd ed.). New York: Marcel Dekker, 1994.

[48] Engles, Warren G., Wang X., and Gan R. Z. "Dynamic Properties of Human Tympanic Membrane After Exposure to Blast Waves." *Annals of Biomedical Engineering* 45, no. 10 (2017): 2383-2394.

[49] Liang, Junfeng, K. D. Smith, H. Lu, T. W. Seale, R. Z. Gan. "Mechanical Properties of the *Papio anubis* Tympanic Membrane: from Infant to Adult." *Annals of Biomedical Engineering*, (2017): under review.

[50] Noyes, Frank R., and Edward S. Grood. "The strength of the anterior cruciate ligament in humans and Rhesus monkeys." *JBJS* 58, no. 8 (1976): 1074-1082.

[51] Lim, D. J. "Human tympanic membrane: an ultrastructural observation." *Acta oto-laryngologica* 70, no. 3 (1970): 176-186.

Appendix A: List of Abbreviations

TM: Tympanic membrane.

G1: Group 1 of baboons age range is less than 1 year old.

G2: Group 2 of baboons age is between 1 and 3 years old.

G3: Group 3 of baboons age is between 3 and 5 years old.

G4: Group 4 of baboons age range is greater than 5 years old.

DMA: Dynamic Mechanical Analyzer.

σ: Stress in MPa calculated by the force (N) divided by the cross-sectional area (mm^2).

ε: Strain (mm / mm) calculated by L / L_0.

λ: Stretch ratio calculated by $1 + \varepsilon$.

SEM: Scanning Electron Microscopy

SE: Standard Error of the Mean

SD: Standard Deviation

FE: Finite element

OCT: Optical coherence tomography

FTS: Frequency-temperature superposition